

Durham Research Online

Deposited in DRO:

13 March 2015

Version of attached file:

Accepted Version

Peer-review status of attached file:

Peer-reviewed

Citation for published item:

Holt, P.J. and Allen, M.B. and van Hunen, J. and Bjørnseth, H.M. (2010) 'Lithospheric cooling and thickening as a basin forming mechanism.', *Tectonophysics.*, 495 (3-4). pp. 184-194.

Further information on publisher's website:

<http://dx.doi.org/10.1016/j.tecto.2010.09.014>

Publisher's copyright statement:

NOTICE: this is the author's version of a work that was accepted for publication in *Tectonophysics*. Changes resulting from the publishing process, such as peer review, editing, corrections, structural formatting, and other quality control mechanisms may not be reflected in this document. Changes may have been made to this work since it was submitted for publication. A definitive version was subsequently published in *Tectonophysics*, 495, 3-4, 3 December 2010, 10.1016/j.tecto.2010.09.014.

Additional information:

Use policy

The full-text may be used and/or reproduced, and given to third parties in any format or medium, without prior permission or charge, for personal research or study, educational, or not-for-profit purposes provided that:

- a full bibliographic reference is made to the original source
- a [link](#) is made to the metadata record in DRO
- the full-text is not changed in any way

The full-text must not be sold in any format or medium without the formal permission of the copyright holders.

Please consult the [full DRO policy](#) for further details.

1
2
3
4 1 Lithospheric cooling and thickening as a basin forming mechanism
5
6

7 2
8
9

10 3 Peter J. Holt^{a*}, Mark B. Allen^a, Jeroen van Hunen^a and Hans Morten Bjørnseth^b.
11 4

12
13 5 ^a Department of Earth Sciences, Durham University, Science Labs, Durham, U.K., DH1 3LE.
14

15 6 ^b Statoil, Forusbeen 50, N-4035 Stavanger, Norway
16

17 7 *Corresponding author, email: p.j.holt@durham.ac.uk
18
19

20 8
21

22 9 ABSTRACT
23
24

25 10
26
27 11 Widely accepted basin forming mechanisms are limited to flexure of the lithosphere, and
28
29 12 lithospheric stretching followed by cooling and thermal subsidence. Neither of these
30
31 13 mechanisms works for a group of large basins, sometimes known as “intracontinental
32
33 14 sags”. In this paper we investigate cooling and thickening of initially thin lithosphere as a
34
35 15 basin forming mechanism, by a combination of forward modelling and a backstripping
36
37 16 study of two Palaeozoic North African basins: Ghadames and Al Kufrah. These are two
38
39 17 of a family of basins, once unified, which lie over the largely accretionary crust of North
40
41 18 Africa and Arabia. Such accretionary crust tends to be juvenile, consisting of
42
43 19 amalgamated island arcs, accretionary prisms and melanges, and typically has near-
44
45 20 normal crustal thicknesses but initially thin mantle lithosphere. Post-accretion subsidence
46
47 21 is modelled using a plate cooling model similar to cooling models for oceanic
48
49 22 lithosphere. The crustal composition and thickness used in the models are varied around
50
51 23 average values of accretionary crust to represent likely heterogeneity. The model allows
52
53 24 the lithosphere to thicken as it cools and calculates the resulting isostatic subsidence.
54
55
56
57
58
59
60
61
62
63
64
65

1
2
3
4
5
6
7
8
9
10
11
12
13
14
15
16
17
18
19
20
21
22
23
24
25
26
27
28
29
30
31
32
33
34
35
36
37
38
39
40
41
42
43
44
45
46
47
48
49
50
51
52
53
54
55
56
57
58
59
60
61
62
63
64
65

25 Water-loaded tectonic subsidence curves from these forward models are compared to
26 tectonic subsidence curves produced from backstripped wells from Al Kufrah and
27 Ghadames basins. A good match between the subsidence curves for the forward model
28 and backstripping is produced when the best estimates for the crustal structure,
29 composition and the present day thickness of the lithosphere for North Africa are used as
30 inputs for the forward model. The model produces sediment loaded basins of 2-7 km
31 thickness for the various crustal assemblies over ~250 Myrs. This shows that lithospheric
32 cooling provides a viable method for producing large basins with prolonged subsidence,
33 without the need for initial extension, provided the condition of initially thin mantle
34 lithosphere is met.

35
36
37

37 **Keywords: basin, lithosphere, subsidence, North Africa**

38

39 **1. Introduction**

40

41 Conventional basin formation mechanisms can be divided into two categories, lithospheric
42 stretching followed by thermal subsidence proportional to the extension (rift basins) and flexure
43 caused by tectonic loading (foreland basins) (Allen and Allen, 2005). However, there is scant
44 evidence for either of these mechanisms forming a group of basins normally classified as
45 “intracontinental sags” – a term that describes their geometry rather than the process of
46 formation. Examples include the Williston and Michigan basins of North America (Klein,
47 1995), the Palaeozoic basins of North African and Arabia (Boote et al., 1998; Konert et al.,

1
2
3
4
5
6
7
8
9
10
11
12
13
14
15
16
17
18
19
20
21
22
23
24
25
26
27
28
29
30
31
32
33
34
35
36
37
38
39
40
41
42
43
44
45
46
47
48
49
50
51
52
53
54
55
56
57
58
59
60
61
62
63
64
65

48 2001); and the Mesozoic Scythian and Turan platforms (Natal'in and Şengör, 2005). The basins
49 are large features, commonly over 1000 km in length, with remarkably uniform, prolonged,
50 gentle subsidence across them, lasting over 200 Myrs. They generally have a polyphase history
51 with a main subsidence phase either preceded or followed by other periods of subsidence and
52 uplift which modify the basin. Armitage and Allen, (2010) recently proposed that these basins
53 are formed by stretching under low strain rates. They argued this based upon the modelling of
54 rifting under low strain rates and the observation that the initiation of subsidence in many
55 intracontinental basins coincides with supercontinent breakup and therefore a broad extensional
56 regime. However, in many basins the evidence for rifting is poor and a number of other
57 mechanisms have been proposed. Subsidence due to cooling of thermal anomalies in the
58 lithosphere has been proposed for the North American intracontinental basins (Kaminski and
59 Jaupart, 2000). The main evidence for this is matching modelling results with the shape and
60 thickness of the present day sedimentary cover. A density change in the crust due to phase
61 changes such as a basalt underplate changing to eclogite has also been suggested based on high
62 velocities in the lower crust interpreted from seismic refraction data (Artyushukov, 2005).
63 However, beneath the Barents/Kara sea region a high density area in the lower crust, suggested
64 by modelling gravity data, has been deemed too local to cause subsidence across the basin.
65 Instead Ritzmann and Faleide, (2009) have suggested that a deeper high velocity zone visible in
66 seismic tomography is evidence of a thick cratonic lithosphere, which causes the subsidence.
67 Heine et al. (2008) noted that many intracratonic basins overlie areas of mantle which have been
68 down welling over the last 100-150 Myrs in their coupled plate and mantle flow model. They
69 proposed that dynamic topography could form these basins. Other subsidence mechanisms and
70 variations on those above have been suggested and are debated in more detail by Armitage and

1
2
3
4 71 Allen (2010) and Klein (1995). It is likely that one mechanism does not explain the formation of
5
6 72 every intercontinental basin and in some cases the basin may be formed by a combination of
7
8
9 73 mechanisms.

10
11 74 Here we show that cooling and thickening of initially thin mantle lithosphere, beneath crust
12
13
14 75 of normal thickness (~30 km) is a viable mechanism for producing basin-scale subsidence. Such
15
16 76 initial conditions are typical of accretionary crust, a term used to summarise the vast orogenic
17
18
19 77 collages of largely juvenile crust and mantle lithosphere, formed by the collision of non-cratonic
20
21 78 terranes: island arcs, accretionary prisms, ophiolites and isolated microcontinents (Murphy and
22
23
24 79 Nance, 1991; Şengör et al., 1993). This would neatly explain the formation of many of the
25
26 80 intracratonic basins on juvenile continental crust such as the Pan African mobile belt or the
27
28
29 81 Scythian and Turan platform. However, we show that where the lithosphere is thinned by a
30
31 82 thermal anomaly it is also possible to form broad, slowly subsiding basins.

32
33 83 This subsidence mechanism is discussed in greater detail in section 2 below, followed by a
34
35
36 84 case study of two of the North African Palaeozoic basins. Thermal subsidence has been
37
38 85 suggested as the cause of intracratonic basins before (Guiraud et al., 2005; Kaminski and
39
40
41 86 Jaupart, 2000; Kominz, 1995). Our contribution is to model the subsidence, compare it to
42
43 87 subsidence in two case studies and to discuss why the lithosphere is plausibly thin in the first
44
45
46 88 place. The subsidence history of the basins is analysed using backstripping. This analysis is
47
48
49 89 compared to results from a numerical forward model of thermal subsidence acting on
50
51 90 accretionary crust, designed to test if it is a mechanism capable of producing the observed
52
53 91 subsidence.

54
55 92

56
57
58 93 **2. Geological background and hypothesis**
59
60
61
62
63
64
65

1
2
3
4
5
6
7
8
9
10
11
12
13
14
15
16
17
18
19
20
21
22
23
24
25
26
27
28
29
30
31
32
33
34
35
36
37
38
39
40
41
42
43
44
45
46
47
48
49
50
51
52
53
54
55
56
57
58
59
60
61
62
63
64
65

94

95 Seismic refraction studies show that present day island arcs can have a crustal thickness of
96 25-35 km, similar to normal continental crust (Holbrook et al., 1999; Takahashi et al., 2007).
97 However, seismic tomography shows slow velocities in the mantle wedge below island arcs
98 which are interpreted as evidence for the presence of melts and thin (~20 km) mantle lithosphere
99 because it is weakened by the addition of fluids from the subducting slab and then eroded by the
100 corner flow in the mantle wedge (Gorbatov et al., 1999; Zhao et al., 1994). This is supported by
101 numerical models of subduction (Arcay et al., 2006; Stern, 2002; van Keken, 2003), by
102 geochemical evidence from the southward initiation of the Philippine subduction zone
103 (Macpherson, 2008) and from the Cascades (Elkins Tanton et al., 2009). These studies suggest
104 an average overall lithospheric thickness of about 50 km beneath island arcs (Fig. 1a).

105 Accretionary prisms may be 30 km thick, largely composed of off-scraped and imbricated
106 fragments of oceanic crust and its sedimentary cover. Whilst subduction is active such prisms
107 are underlain by the oceanic plate. When subduction has recycled the oceanic plate in to the
108 mantle, the base of the prism may be in contact with the asthenosphere, particularly if ocean
109 closure resulted in the collision of two such prisms, initially on opposite sides of the ocean,
110 rather than collision of the prism with a continental margin. The Cenozoic East Anatolian
111 Accretionary Complex may be an example of such a lithospheric structure, where tomographic
112 studies suggest a thin or even absent mantle lithosphere (Zor et al., 2003).

113 A notable feature of accretionary orogenic belts is that they lack evidence for substantial
114 crustal thickening (and presumably lithosphere thickening): there is rarely evidence for pre-
115 collision passive continental margins, Alpine-type nappes, or overfilled foreland basins
116 (“molasse”) (Şengör and Okurogullari, 1991). This means that putative lithospheric

1
2
3
4
5
6
7
8
9
10
11
12
13
14
15
16
17
18
19
20
21
22
23
24
25
26
27
28
29
30
31
32
33
34
35
36
37
38
39
40
41
42
43
44
45
46
47
48
49
50
51
52
53
54
55
56
57
58
59
60
61
62
63
64
65

117 delamination following an orogeny of this type, hypothesised by Ashwal and Burke, (1989), is
118 not our preferred mechanism for thinning the lithosphere. However, it would produce similar
119 starting conditions to those in our model.

120 As accretionary crust is assembled through subduction and collision, the thin mantle
121 lithosphere of the original terranes is inherited by the final collage (Fig. 1b). We hypothesise
122 that once accretion is completed, and subduction has ceased beneath an area, the underlying
123 asthenosphere will cool, thickening the mantle lithosphere. This cooling will cause prolonged
124 subsidence, forming basins (Fig. 1c).

125 *Figure 1 should be placed here*

126 Our model is similar to the thermal subsidence phase of McKenzie style rifting (McKenzie,
127 1978) or the subsidence of the ocean floor away from a mid ocean ridge, except that the crust
128 involved is continental, albeit juvenile, and has not been thinned in any way. In this paper we
129 proceed to show how this mechanism could produce the basins in North Africa. However, there
130 are many other intracratonic basins on accreted crust where this mechanism could apply. Table
131 1 provides a sample of some of the basins we aware of, but is by no means an exhaustive list.
132 Allen and Armitage, (in press) note a clustering in time of the initiation of intracratonic basins
133 which they link to the breakup of supercontinents. In Table 1 we show the start of subsidence
134 follows closely the end of accretion and the clustering may be related to the end of periods of
135 accretion of crust. The basins are long lived features and so many have later phases of
136 subsidence which potentially have other causes.

137 *Table 1 should be placed here.*

138

139 **3. Tectonic subsidence history of backstripped North African basins**

1
2
3
4
5
6
7
8
9
10
11
12
13
14
15
16
17
18
19
20
21
22
23
24
25
26
27
28
29
30
31
32
33
34
35
36
37
38
39
40
41
42
43
44
45
46
47
48
49
50
51
52
53
54
55
56
57
58
59
60
61
62
63
64
65

140
141
142
143
144
145
146
147
148
149
150
151

In order to test whether the proposed mechanism of subsidence provides a good explanation for anomalous basins developed over accretionary crust, subsidence histories for the Ghadames and Al Kufrah basins were investigated using backstripping. These are Palaeozoic basins situated on the North African crust, which was accreted in the Pan African orogeny during Neoproterozoic times (Caby, 2003; Stern, 1994). Most of the basement to North Africa and Arabia is juvenile, generated and assembled during the Pan African orogeny. The western margin is the West African Craton. The southern limit is the Congo Craton. The eastern and northern limits are not so well defined because of later rifting and collision with Eurasia. For example, similar basement underlies much of the territory of Iran, but with a more complicated Mesozoic and Cenozoic magmatic and tectonic history. The outcrop or sub-Mesozoic subcrop of the Palaeozoic strata of North Africa and Arabia is shown in Fig. 2.

Figure 2 should be placed here

152
153
154
155
156
157
158
159
160
161
162

The proportion of cratonic nuclei within this vast, 10,000,000 km² orogen is debated, but plausibly is small. There are indications of pre Late Proterozoic crust within North Africa, based on Meso- or Palaeo-Proterozoic isotopic model ages and detrital zircons in younger metamorphic terranes (Black et al., 1993; Sultan et al., 1990). But the Late Proterozoic tectonic overprint is severe, suggesting that extensive magmatic and metamorphic re-working and additions took place during the Pan African orogeny, and no single, regionally extensive block survived the Late Proterozoic orogeny with its original structure and boundaries preserved. A significant re-worked region has been called the Saharan metacraton (Abdelsalam et al., 2002), but this is not recognised by all workers e.g. (Bumby and Guiraud, 2005). Whatever the nature and origins of the Saharan metacraton, it appears to have had little impact on the overlying

1
2
3
4
5
6
7
8
9
10
11
12
13
14
15
16
17
18
19
20
21
22
23
24
25
26
27
28
29
30
31
32
33
34
35
36
37
38
39
40
41
42
43
44
45
46
47
48
49
50
51
52
53
54
55
56
57
58
59
60
61
62
63
64
65

163 Phanerozoic basins (Fig. 2). These are continuous across the metacraton margins, without
164 discernible change in sedimentary thickness or composition.

165 The end of the Pan African orogeny was diachronous. Local timings for the last deformation
166 vary from Late Precambrian to the Early Cambrian e.g. (Paquette et al., 1998). Present-day
167 lithosphere thickness across North Africa is on the order of ~100 km (Pasyanos and Nyblade,
168 2007; Priestley and McKenzie, 2006); except for the West African Craton where it reaches >200
169 km. Crustal thicknesses are not well-constrained, but are variously estimated at 30 to 40 km
170 thick from gravity and seismic interpretations (Seber et al., 2001), or 25 to 35 km from the
171 inversion of surface waves (Pasyanos and Nyblade, 2007).

172 The Ghadames Basin is well studied because large hydrocarbon accumulations have been
173 discovered within it (Echikh, 1998). Several wells have penetrated the crystalline basement and
174 there are large amounts of seismic data for the basin. This means the geometry of the basin is
175 well understood. This allows the most complete stratigraphic sections to be identified, which is
176 helpful when backstripping. The Al Kufrah Basin is less well studied and has only two
177 published wells which reached the crystalline basement (Grignani et al., 1991). To a first order,
178 it has a similar Palaeozoic stratigraphy to the Ghadames Basin. Enough data are available for Al
179 Kufrah to make it viable for modelling.

180

181 *3.1 Methodology*

182

183 Backstripping is a well known technique for calculating the tectonic subsidence of a
184 particular horizon in a basin over time. We use the basement/cover boundary, which reveals the
185 overall subsidence (Allen and Allen, 2005; Sclater and Christie, 1980). The technique first

1
2
3
4
5
6
7
8
9
10
11
12
13
14
15
16
17
18
19
20
21
22
23
24
25
26
27
28
29
30
31
32
33
34
35
36
37
38
39
40
41
42
43
44
45
46
47
48
49
50
51
52
53
54
55
56
57
58
59
60
61
62
63
64
65

186 decompacts each sedimentary layer through time. This gives the total subsidence curve for the
187 basement which is assumed to be composed of the tectonic subsidence, the isostatic effect
188 (weight) of the sediments and the changes in water depth compared to the present day sea level.
189 The effects of the sediments and sea level changes are removed so that the remaining subsidence
190 is due purely to the tectonic driving force. A global eustatic sea-level curve of (Haq and
191 Schutter, 2008) is used to remove the effects of sea-level changes.

192 The backstripping method assumes that the compaction of the sediments is purely
193 mechanical (due to the weight of the sediments above) and ignores chemical processes, such as
194 cementation, which are very difficult to take into account because they depend on a complex
195 series of factors such as fluid flow, composition, temperature and pressure. Backstripping
196 assumes that the sediments are laid down in successive layers throughout time and does not take
197 into account periods of uplift and erosion or non deposition. These are difficult to include in
198 backstripping because generally the amount of eroded material is poorly constrained. If the
199 present day burial depth of the basement is the deepest it has been, then any erosion will make
200 no difference because the sediments are at their peak pressure. Otherwise the compaction of the
201 sediments will be underestimated. There are no porosity depth relationships available for the
202 sediments in North Africa and we use standard relationships from published work (Sclater and
203 Christie, 1980). We assume that the compaction curves, which are based on sediments from the
204 North Sea, are applicable to the sediments in North Africa. This is justifiable because the North
205 African sediments are entirely siliciclastic and are similar to those in the North Sea.

206 This method was applied to a composite well from the Ghadames Basin. A composite well
207 was used because it gives the most complete section possible from the basin therefore showing
208 the maximum subsidence and limiting the effect of erosion. The composite well was created

1
2
3
4
5
6
7
8
9
10
11
12
13
14
15
16
17
18
19
20
21
22
23
24
25
26
27
28
29
30
31
32
33
34
35
36
37
38
39
40
41
42
43
44
45
46
47
48
49
50
51
52
53
54
55
56
57
58
59
60
61
62
63
64
65

209 using four unpublished wells from the transect shown on Fig. 2, to identify the most complete
210 sections and to ensure that the differences in the thickness of the layers were due to variations in
211 erosion rather than deposition rates. This minimises the errors related to eroded sections of the
212 stratigraphy. It also produces a subsidence curve which emphasises the subsidence phases rather
213 than any uplift. This allows us to see clearly the main subsidence phase associated with basin
214 formation, rather than later phases of uplift or subsidence. This approach was not possible in the
215 Al Kufrah Basin because of the scarcity of available well data, and instead the backstripping
216 methodology was applied directly to the two available wells.

217

218 *3.2 General Stratigraphy*

219

220 Detailed descriptions of the stratigraphy in the Ghadames, Al Kufrah and other North African
221 basins can be found in papers such as Bellini and Massa (1980), Echikh (1998), Fekirine and
222 Abdallah (1998), Grignani et al. (1991) and Lüning et al. (1999). Therefore we present a brief
223 summary of the evolution of the Palaeozoic basins on the accretionary crust of North Africa
224 collated from Boote et al. (1998), Bumby and Guiraud (2005), Craig et al. (in press), Guiraud
225 and Bosworth (1999) and Guiraud et al. (2005) alongside more detailed observations from the
226 basins themselves. The basins are filled with a largely siliciclastic succession with some
227 evaporites and carbonates towards the end of the Palaeozoic. The whole of North Africa
228 subsided as a large platform from roughly the start of the Palaeozoic, depositing a wedge of
229 sediments that thinned to the south (Selley, 1997). Only localised Late Proterozoic/Early
230 Palaeozoic rifting is known (see Fig. 6 of Guiraud et al. (2005), and as several of the main
231 basins are mature in terms of hydrocarbon exploration it is unlikely that major rifts have been

1
2
3
4
5
6
7
8
9
10
11
12
13
14
15
16
17
18
19
20
21
22
23
24
25
26
27
28
29
30
31
32
33
34
35
36
37
38
39
40
41
42
43
44
45
46
47
48
49
50
51
52
53
54
55
56
57
58
59
60
61
62
63
64
65

missed. Seismic lines through the Kufrah Basin show Late Proterozoic/Cambrian rifts (Lüning et al., 1999), however these are only seen on seismic lines in the south of the basin (Ghanoush and Abubaker, 2007) and do not explain subsidence across the whole basin or in neighbouring basins. Nor do the dimensions of the subsiding area ($\gg 1000$ km) fit a flexural, foreland basin mechanism. In any case, there is no record of an appropriate orogeny lasting through the Palaeozoic along the Gondwanan continental margin (Stampfli and Borel, 2002). The initial sediments are largely fluvial sandstones and conglomerates in the Cambrian, changing to marine sandstones in the early Ordovician. The Cambrian age for the earlier sediments is inferred because there are very few trace fossils to date the sediments until the marine incursions (Grignani et al., 1991). In the mid to late Ordovician there was major glaciation creating a regional erosional surface (Le Heron et al., 2010). The amount of erosion varies greatly reflecting the geometry of the ice sheets. Locally in Al Kufrah the erosion cuts down to the Cambrian, but in other areas a complete section to the Mid Silurian is preserved. In these areas the erosion is minimal and the glaciation reflects a period of non deposition. The erosion becomes less severe to the north into the Murzuq and Ghadames basins (Bellini and Massa, 1980; Fekirine and Abdallah, 1998).

Coarse to medium grained sandstones and tillites related to the retreat of the glaciers were deposited at the end of the Ordovician. This was followed by a major marine transgression leading to the deposition of shales throughout the Early Silurian, but water depths decreased with time and the shales grade up to shoreface sandstones. The shales at the base of the Silurian are one of the main source rocks and record the maximum water depth experienced by the basins during the Palaeozoic. Turner (1978) interpreted it as a shallow shelf environment with water depths of about 200 m. Separation of individual basins began during the Silurian caused

1
2
3
4
5
6
7
8
9
10
11
12
13
14
15
16
17
18
19
20
21
22
23
24
25
26
27
28
29
30
31
32
33
34
35
36
37
38
39
40
41
42
43
44
45
46
47
48
49
50
51
52
53
54
55
56
57
58
59
60
61
62
63
64
65

255 by a period of compression most likely related to the Acadian collision (Guiraud and Bosworth,
256 1999). This resulted in an unconformity across the basins of North Africa, but within basins it is
257 localised over arches, such as uplift of the arch between the Ghadames and Murzuq basins
258 (Boote et al., 1998). During the Devonian the basins were filled with shallow marine sandstones
259 and siltstones, and fluvial sandstones, corresponding to fluctuations in sea-level. The
260 transgressions and regressions, as well as prograding systems, can be correlated between basins
261 (Bellini and Massa, 1980). The southern basins (i.e. Al Kufrah) show a greater continental
262 influence compared with the basins further to the north (i.e. Ghadames) (Boote et al., 1998).

263 Deposition at the start of the Carboniferous was similar to the Devonian, with variations in
264 siliciclastic sediments controlled by sea-level changes, but with some carbonates deposited
265 locally in the Ghadames Basin (Fekirine and Abdallah, 1998). The Palaeozoic sediments were
266 terminated by the Late Carboniferous-Permian Hercynian orogeny, which was an important
267 period of compression, causing uplift along the flanks of many of the basins and forming much
268 of the Palaeozoic subcrop pattern seen in Fig 2. In some areas, such as beneath the Sirte Basin, it
269 eroded down to the Cambrian sediments (Abadi et al., 2008). Mesozoic and Cenozoic tectonics
270 related to the opening and closing of Tethys to the north of North Africa, and the opening of the
271 Atlantic Ocean, modified some of the basin geometries and subsidence patterns. **The Sirte Basin**
272 **began forming as a rift basin during the late Cretaceous (100-70 Myrs), and continued to the**
273 **Early Eocene. Extension was due to far-field stresses related to changes in the spreading rate of**
274 **the Central and South Atlantic (Guiraud et al., 2005; Janssen et al., 1995). However, this has**
275 **recently been challenged by Capitano et al. (2009) who suggest this does not fit the timing of**
276 **extension, and that a better explanation is that the African plate was placed under tensile stress**
277 **by avalanching of its subducted northern edge through the 660 km discontinuity, beneath the**

1
2
3
4
5
6
7
8
9
10
11
12
13
14
15
16
17
18
19
20
21
22
23
24
25
26
27
28
29
30
31
32
33
34
35
36
37
38
39
40
41
42
43
44
45
46
47
48
49
50
51
52
53
54
55
56
57
58
59
60
61
62
63
64
65

278 **Hellenic arc.** This basin borders the Murzuq and Al Kufrah basins, but was formed later, and so
279 is not analogous to the basins specifically considered in this study. **There is little evidence of**
280 **similar extension in the surrounding basins at this period as shown by the thickness of the**
281 **Cretaceous deposits seen in the wells from Fig. 4.** Similar Palaeozoic successions are seen in the
282 Reggane, Ahnet and Tindouf basins to the north of the West African Craton (Boote et al., 1998).
283 The major event affecting the Paleozoic basins is the Alpine unconformity caused by uplift
284 related to collision of Africa and Europe at the end of the Eocene. See Brunet and Cloetingh
285 (2003) and papers therein for descriptions of the Carboniferous-Recent evolution of basins
286 within northern North Africa and Arabia. These events uplifted the basin margins, and in some
287 areas obscured the earlier subsidence by removing significant thicknesses of sediments. Much of
288 the erosion is focused on the flanks of the basins, although some does occur within the basins, as
289 evidenced by missing Carboniferous section in the well A1 from Al Kufrah (Fig 3). We have
290 sought to minimise the effects of erosion as outlined in our methodology. Details of the
291 stratigraphy for the three wells which were backstripped are shown in Fig. 3.

292 *Figure 3 should be placed here*

294 3.3 Results

296 Fig. 4 shows the tectonic subsidence profiles derived from the backstripping. The profiles
297 start at the beginning of the Cambrian, but the precise time of the onset of subsidence is poorly
298 constrained because the sediments are fluvial sandstones, with no fossils. The subsidence rates
299 are fairly rapid to begin with and slow gradually through time with little or no tectonic
300 subsidence during the Mesozoic and Cenozoic (fastest rates are 22.2 m/Myr in Ghadames and

1
2
3
4
5
6
7
8
9
10
11
12
13
14
15
16
17
18
19
20
21
22
23
24
25
26
27
28
29
30
31
32
33
34
35
36
37
38
39
40
41
42
43
44
45
46
47
48
49
50
51
52
53
54
55
56
57
58
59
60
61
62
63
64
65

301 10.1 m/Myr in Al Kufrah). The subsidence profiles are steadily decaying curves without clearly
302 separate rift and thermal subsidence phases, i.e. they resemble the thermal subsidence that
303 typically follows rifting, without a rift phase being apparent. **The subsidence curves show very**
304 **little tectonic subsidence affected the basins after 250 Myrs, showing that later periods of**
305 **subsidence, such as that in the Sirte basin, only slightly modified the Ghadames and Al Kufrah**
306 **basins.** The tectonic subsidence is not smooth; the curves show the periods of erosion and uplift
307 evident in the sedimentary record, e.g. Late Palaeozoic, Hercynian, uplift.

308 *Figure 4 should be placed here*

309 Both basins show very similar tectonic subsidence patterns, both in the timing and the
310 amount of the tectonic subsidence. This is evidence that one causal mechanism generated the
311 Palaeozoic subsidence across North Africa. The total tectonic subsidence in the Ghadames
312 composite well is ~2230 m. This is similar to the ~1740 m of subsidence calculated for the
313 B1NC43 well in the Al Kufrah Basin. As Fig. 4 shows, well A1NC43 appears to have had less
314 subsidence (~1260 m). However much of the Carboniferous stratigraphy has been removed by
315 the Hercynian deformation, so this lower total is plausibly an effect of erosion rather than
316 differential subsidence.

317 The uncertainties involved come from the input parameters and the assumptions. These
318 include the thickness and depths of the sedimentary layers from errors in picking horizons from
319 well logs or due to erosion. Estimates of these are not provided by Grignani et al. (1991).
320 Assuming that compaction is entirely mechanical also introduces uncertainties. The errors from
321 using the general compaction curves were estimated by carrying out the backstripping with the
322 entire sedimentary column being made of either shale or sandstones which form the two end
323 members of the compaction curves (Sclater and Christie, 1980). Depositional water depth can

1
2
3
4
5
6
7
8
9
10
11
12
13
14
15
16
17
18
19
20
21
22
23
24
25
26
27
28
29
30
31
32
33
34
35
36
37
38
39
40
41
42
43
44
45
46
47
48
49
50
51
52
53
54
55
56
57
58
59
60
61
62
63
64
65

324 contribute to large uncertainties because it is difficult to tell the depth of sediments deposited in
325 deep water. As shown in section 3.2, in the basins in North Africa this is not such an issue
326 because all sediments were deposited in shallow waters less than 200 m (Grignani et al., 1991).
327 The uncertainties in water depth estimates for shallow water sediments are much smaller (10s of
328 meters). There are also errors related to corrections for the eustatic sea-level. The largest sea-
329 level fluctuations do not exceed 200 m, so the uncertainties in water depths and eustatic sea-
330 level will have little effect on the overall shape of the curves. The errors from the backstripping
331 calculations are shown as the dashed lines in Fig. 4. The errors make a negligible difference to
332 both the shape of the curves and the overall amount of subsidence.

333

334 **4. Forward Modelling**

335

336 Numerical forward modelling of basement subsidence was used to test whether lithospheric
337 cooling and growth is a realistic mechanism for the subsidence of accretionary crust. This is
338 compared to the backstripped results from basins in North Africa to determine if it fits the
339 observed subsidence. The modelling was carried out using Matlab and the code was tested
340 against analytical solutions.

341

342 *4.1 Methodology of the forward modelling*

343

344 The numerical subsidence model is based on and tested against the plate models for sea floor
345 spreading (Parsons and Sclater, 1977; Stein and Stein, 1992). It is modified to include layered
346 continental crust with radioactive heat production. It solves the vertical conductive heat flow

1
2
3
4 347 through a one-dimensional column of the lithosphere and upper mantle.

5
6
7 348
$$\rho C_p \frac{\partial T}{\partial t} = \frac{\partial}{\partial z} \left(k \frac{\partial T}{\partial z} \right) + A \quad (1)$$

8
9

10 349 Equation 1 is solved using a finite difference technique with a grid resolution of 1 km. T is
11
12 350 the temperature of the rock at a particular point in the grid at depth z . A is the contribution of
13
14 351 radioactive heat production and t is the time over which the temperature is changing. Time-
15
16 352 stepping is performed with an Euler forward time-integration scheme. The material properties of
17
18 353 the rock are the thermal conductivity (k), the specific heat capacity (C_p) and the density (ρ). The
19
20 354 density of the rock is dependant on the temperature and is calculated using equation 2.
21
22

23
24
25 355
$$\rho = \rho_0 (1 - \alpha(T - T_0)) \quad (2)$$

26
27

28 356 In equation 2 the reference density (ρ_0) and the coefficient of thermal expansion (α) are
29
30 357 dependant on the rock type (Turcotte and Schubert, 2002). The values used for all the
31
32 358 parameters in equations 1 and 2 are shown in Fig. 5.
33
34

35 359 *Figure 5 should be placed here*
36

37
38 360 The model is set up with a two layer crust composed of a felsic upper crust and granulitic
39
40 361 lower crust which is underlain by mantle lithosphere. The base of the lithosphere is purely
41
42 362 thermal rather than compositional and describes the temperature below which the mantle rock
43
44 363 does not deform significantly over geological timescales. The 1200 °C isotherm is used
45
46 364 (Turcotte and Schubert, 2002). The model starts with a 20 km thick mantle lithosphere, which
47
48 365 matches the starting conditions described in section 2. The temperature at the surface of the
49
50 366 model is set as 0°C. The temperature at the base of the model is calculated using a potential
51
52 367 temperature at the surface using an adiabatic gradient of 0.3°C per km. Constant temperature
53
54 368 boundary conditions are used at the top and bottom of the model. The initial temperature
55
56 369 conditions follow the mantle adiabat to up to a transition point 20 km below the crust above
57
58
59
60
61
62
63
64
65

1
2
3
4
5
6
7
8
9
10
11
12
13
14
15
16
17
18
19
20
21
22
23
24
25
26
27
28
29
30
31
32
33
34
35
36
37
38
39
40
41
42
43
44
45
46
47
48
49
50
51
52
53
54
55
56
57
58
59
60
61
62
63
64
65

370 which they follow a linear gradient to the surface. The depth and therefore temperature at this
371 transition point is dependent on the thickness of the crust and the potential temperature for the
372 surface. The initial conditions for the model are shown in Fig. 5. The temperature profile is used
373 to calculate the density at grid point in the column from the reference density using equation 2.
374 The elevation is calibrated from the density profile of the column using a column of hot mid
375 ocean ridge material with a 7 km thick basaltic-gabbroic crust at 3 km below sea-level as
376 reference. Standard Pratt isostasy (Allen and Allen, 2005) is used. When the topography of the
377 model drops below sea level the basin is filled with water. The thermal boundary condition is
378 applied to the basement floor because water in the basin would have an almost uniform
379 temperature due to convection. However, the water is included in the isostasy so the model
380 effectively produces water loaded tectonic subsidence.

381 One inherent weakness of the plate model is that it only calculates the heat transfer by
382 conduction (Parsons and Sclater, 1977). At the base of the plate heat transfer changes from
383 conduction to convection (Huang et al., 2003; Richter and Parsons, 1975; van Hunen et al.,
384 2005). The plate model does not explicitly describe the physics of this transition, but provides a
385 very good fit to the bathymetry and heatflow data (Huang and Zhong, 2005) and included
386 references. It does not help explain the physical process that causes the thermal boundary layer
387 to become stable at this depth. We ignore the temperature dependence of k , C_p and α . This
388 assumption slightly overestimates temperatures in the top half of the model and underestimates
389 temperatures in the bottom half of the model (McKenzie et al., 2005). This means the depth to
390 the base of the lithosphere is an upper limit.

391

392 *4.2 Results: Effects of varying parameters and the best fit model for the backstripping*

1
2
3
4
5
6
7
8
9
10
11
12
13
14
15
16
17
18
19
20
21
22
23
24
25
26
27
28
29
30
31
32
33
34
35
36
37
38
39
40
41
42
43
44
45
46
47
48
49
50
51
52
53
54
55
56
57
58
59
60
61
62
63
64
65

393

The model is set up so that the each of the parameters from equation 1 can be changed and the structure of the model, shown in Fig. 5, can be altered. Changing these will alter the subsidence produced. It is important to understand how these different parameters affect the subsidence before trying to find the best fitting model because there may be a trade off between different parameters.

399

The model is most sensitive to changes in the thickness of the crust and the plate thickness because they change the isostacy by varying the amount of low density crust and high density lithosphere. However, changing the plate thickness affects the timing of the subsidence whereas changing the crustal thickness only affects the total subsidence so their effects can be distinguished. There is not a direct trade-off between the two parameters. The model is less sensitive to variations in the potential temperature and radioactive heat production respectively (Fig. 6). In each case only the parameter under investigation is changed and the estimates for North African crust shown in Fig. 5 are used as the default the parameters. The amount of variation in the input parameters is based on the uncertainties and variation across North Africa from the literature. The present day thickness of the crust of North Africa was calculated to be between 30 and 40 km thick from low resolution gravity and seismic interpretations and gravity modelling in the 3-D crustal model of Seber et al. (2001) over the area of interest. This is thicker than the crustal thickness of 25-35 km estimated from the inversion of surface waves given by Pasyanos and Nyblade (2007). Due to the uncertainty in crustal thickness our model calculations were run for a range of crustal assemblages between 20 and 40 km thick. The results are shown in Fig. 6a. With a crustal thickness of 40 km, ~ 1.2 km of tectonic subsidence takes place, however the crust is too buoyant to drop below sea-level, so no basin is formed. When the crust

1
2
3
4
5
6
7
8
9
10
11
12
13
14
15
16
17
18
19
20
21
22
23
24
25
26
27
28
29
30
31
32
33
34
35
36
37
38
39
40
41
42
43
44
45
46
47
48
49
50
51
52
53
54
55
56
57
58
59
60
61
62
63
64
65

416 is reduced to 36 km thick the total subsidence increases to ~1.9 km and 1 km of water loaded
417 tectonic subsidence is recorded. A 20 km thick crust starts at 1.4 km below sea-level and
418 experiences ~2.7 km of tectonic subsidence as the lithosphere cools and thickens. There have
419 been no deep crustal seismic lines of North Africa published so the proportion of upper crust
420 and lower crust is unknown. Therefore the model was run with a 30 km thick crust where the
421 thickness of the upper crust was varied between 10 and 20 km. This alters the total subsidence
422 by about 500 m. A 1 km decrease in the total crustal thickness causes ~150 m of additional
423 subsidence, whereas changing 1 km of upper crust to lower crust only increases the total
424 subsidence by ~ 50 m. The main reason both these parameters affect the overall subsidence is
425 that they change the isostasy by varying the amount of low density crust. In all these scenarios
426 the timing of the subsidence does not change, most of the subsidence occurs in the first 100
427 Myrs and the subsidence after 200 Myrs is negligible.

Figure 6 should be placed roughly here in the text

429 We also change the amount of radiogenic heat production. Estimations of heat production in
430 the continental crust vary between 1.31 mWm^{-3} and 0.8 mWm^{-3} for the upper crust and 1.0
431 mWm^{-3} and 0.6 mWm^{-3} for the lower crust. The values reflect calculations of bulk crustal heat
432 production from the literature (Christensen and Mooney, 1995; Gao et al., 1998; Shaw et al.,
433 1986; Wedepohl, 1995). Changing the heat production for the upper and lower crust between
434 these extremes causes a small variation of 100 m in the tectonic subsidence. The heat production
435 of the bulk continental crust will be lower than that of accretionary crust and heat production
436 would have been higher during the Palaeozoic, so the model was also run with a higher heat
437 production of 2.0 mWm^{-3} (upper crust) and 1.2 mWm^{-3} (lower crust). This does reduce the
438 overall amount of tectonic subsidence from ~ 1800 to 1550m, but does not alter the timing. Fig.

1
2
3
4
5
6
7
8
9
10
11
12
13
14
15
16
17
18
19
20
21
22
23
24
25
26
27
28
29
30
31
32
33
34
35
36
37
38
39
40
41
42
43
44
45
46
47
48
49
50
51
52
53
54
55
56
57
58
59
60
61
62
63
64
65

439 6b shows that varying the heat production in the crust has a small effect compared to varying the
440 crustal thickness.

441 The other main parameter which has a big effect on the subsidence is the thickness of the
442 model, referred to as the plate thickness (Fig. 6c). A plate thickness of 95 km, which is the
443 preferred for the oceanic lithospheric cooling model of Stein and Stein (1992) results in 200 m
444 of subsidence, of which 80% has occurred within ~70 Myrs, with a final lithospheric thickness
445 (i.e. depth to the 1200 °C isotherm) of 81.1 km. At the other extreme when a plate thickness of
446 200 km is used, similar to an Archean craton (Priestley and McKenzie, 2006), ~3050 m of
447 subsidence is produced, and it takes longer for the subsidence to tail off. 80% of the subsidence
448 is completed within 200 Myrs. The lithosphere thickness after 500 Myrs is 166.5 km. As the
449 plate thickness is increased the final lithospheric thickness also increases. A thicker, dense
450 lithosphere results in more subsidence, occurring over a longer time period.

451 The temperature at the base of the plate is controlled by both the potential temperature at the
452 surface (the temperature at which the mantle adiabat dissects the surface) and the thickness of
453 the plate (Fig. 5). Increasing the potential temperature by 1°C increases the temperature at the
454 base of the plate by 1°C whereas increasing the thickness of the model causes the temperature at
455 the base of the plate to increase along the mantle adiabat i.e. 3°C for every 10 km. The potential
456 temperature was varied from 1280 °C, which was suggested by McKenzie et al. (2005) to 1410
457 °C suggested by Parsons and Sclater (1977). As Fig. 6d shows this variation of 100 °C in the
458 potential temperature produces less than 500 m difference in the overall subsidence.

459 Van Wees et al. (2009) report a trade off between parameters, such as the final lithospheric
460 thickness (plate thickness) and crustal thickness, when investigating the uncertainties in surface
461 heatflow using modelling. However, in this study we find that varying the plate thickness to fit

1
2
3
4
5
6
7
8
9
10
11
12
13
14
15
16
17
18
19
20
21
22
23
24
25
26
27
28
29
30
31
32
33
34
35
36
37
38
39
40
41
42
43
44
45
46
47
48
49
50
51
52
53
54
55
56
57
58
59
60
61
62
63
64
65

462 the time span of the subsidence and then varying the crustal thickness to fit the amount of
463 subsidence allows a unique solution to be obtained for these parameters. However, there is a
464 direct trade off between the crustal thickness, heat production and potential temperature because
465 they all only affect the total subsidence. The model is not sensitive to reasonable variations in
466 the heat production or potential temperature, but is sensitive to variations in crustal thickness
467 suggested for North Africa. Therefore the trade off between these parameters is not important
468 when trying to fit the modelled subsidence to the observed subsidence.

469 The sensitivity of the model to k , C_p and α was also investigated, but because much less is
470 known about the amount of variation that is found in the crust they are not discussed here and
471 the standard values from the literature (Fig. 5) are used. The forward model produces significant
472 subsidence for a large variety of crustal assemblages and for wide variation in the parameters. It
473 supports the hypothesis that lithospheric cooling and thickening caused the subsidence seen
474 across North Africa.

475
476 **5. Discussion**

477
478 *5.1 Comparison of tectonic subsidence from backstripping and forward modelling.*

479
480 The results of the forward modelling show a good fit to the backstripping from both basins as
481 demonstrated by Fig. 7. Four forward model runs are shown on the diagram. One of which uses
482 the best estimates for the crustal assemblage, thickness and plate thickness from the literature,
483 one which is the best fit to the backstripping and then two runs which show the maximum and
484 minimum subsidence for reasonable variations of the properties of the North African crust.

1
2
3
4 485 The forward model curves are smooth unlike the backstripped subsidence curves. This is
5
6 486 because North African crust has experienced periods of uplift, and the forward model doesn't
7
8
9 487 include these complexities. However, the forward model fits the broad shape of the backstripped
10
11 488 subsidence curve very well. Both have a concave up shape, and the timescale and magnitude of
12
13
14 489 subsidence are very similar. When the crustal thickness, final lithosphere thickness and heat
15
16 490 production used are taken from the best estimates of the North African crust in the literature
17
18
19 491 (Fig. 5), and therefore are independent of the backstripping, the forward model curve only
20
21 492 underestimates the subsidence slightly, by <500 m in 350 Myrs. The discrepancy at 500 Myrs is
22
23
24 493 ~700 m, because of the Mesozoic and Cenozoic subsidence of the Ghadames Basin. This is a
25
26 494 separate tectonic event, related to Tethyan opening and evolution (Guiraud and Bosworth,
27
28
29 495 1999). The best fit model has been fitted iteratively by eye. The input parameters for the best fit
30
31 496 model are the same as those from the literature except that the plate is 155 km thick, which
32
33 497 results in a final lithospheric thickness of ~124 km. The crust beneath the basins cannot be
34
35
36 498 assumed to be homogenous, in fact because it is accreted from numerous crustal fragments it is
37
38 499 likely that it varies across North Africa. The maximum and minimum subsidence based on the
39
40
41 500 variation found in the literature, discussed in section 4.2, is shown in Fig. 7. The upper limit has
42
43 501 a 35 km thick crust with 30 km of upper crust and 5 km of lower crust, a heat production of 1.6
44
45 502 mWm^{-3} in the upper crust and 1.0 mWm^{-3} in the lower crust, a potential temperature of 1280 °C
46
47
48 503 and plate thickness of 120 km. The lower limit has 25 km thick crust, where the top 5 km is
49
50
51 504 upper crust and the rest is lower crust, a heat production of 1.0 mWm^{-3} in the upper crust and 0.6
52
53 505 mWm^{-3} in the lower crust, a potential temperature of 1380 °C and a plate thickness of 180 km.

54
55 506 *Figure 7 should be placed here*
56
57
58
59
60
61
62
63
64
65

1
2
3
4
5
6
7
8
9
10
11
12
13
14
15
16
17
18
19
20
21
22
23
24
25
26
27
28
29
30
31
32
33
34
35
36
37
38
39
40
41
42
43
44
45
46
47
48
49
50
51
52
53
54
55
56
57
58
59
60
61
62
63
64
65

507 There are a number of assumptions in both the modelling and backstripping. Both are
508 oversimplified versions of the real situations and processes. The problem has been simplified to
509 be one dimensional, whereas the basins are three dimensional features. We assume that the
510 basins are large enough features that it is possible to remove effects of marginal uplift from the
511 sedimentary record by choosing wells away from the basin flanks, or constructing composite
512 wells. This allows the basins to be treated as one dimensional features. Another assumption is
513 that North African crust resembles the starting conditions outlined in the hypothesis. This is
514 difficult to test as there is no newly assembled accretionary orogenic belt on the North African
515 scale that can be used as an analogue. However, the building blocks of accretionary crust are
516 available to study. It seems reasonable that North African crust formed through subduction
517 would share the thin lithosphere of its component island arcs and accretionary wedges. When
518 North African crust is modelled using these starting conditions it produces a good fit to the
519 subsidence. As mentioned in the hypothesis as long as the crust is of near normal thickness and
520 has a thin mantle lithosphere these results still apply. The two North African basins have been
521 chosen as case studies, but we propose that the lithosphere cooling and thickening hypothesis is
522 applicable to all the Palaeozoic basins on the accretionary crust of North Africa and Arabia, and
523 to other basins on accretionary crust around the world, such as the Mesozoic cover of the
524 Scythian and Turan platforms of SW and Central Asia (Natal'in and Şengör, 2005), the
525 Mesozoic cover of the Tasmanides of Eastern Australia (Gallagher et al., 1994) and the late
526 Palaeozoic platform cover over the Altaid orogenic collage in Central Asia (Cook et al., 1994).

527 The good fit between modelled and backstripped subsidence curves do not prove that
528 lithosphere thickening and cooling is the cause of the subsidence. Other authors have suggested
529 that the Palaeozoic basins in North Africa formed by rifting (Lüning et al., 1999), orogenic

1
2
3
4
5
6
7
8
9
10
11
12
13
14
15
16
17
18
19
20
21
22
23
24
25
26
27
28
29
30
31
32
33
34
35
36
37
38
39
40
41
42
43
44
45
46
47
48
49
50
51
52
53
54
55
56
57
58
59
60
61
62
63
64
65

collapse (Ashwal and Burke, 1989) and dynamic topography (Heine et al., 2008). Lüning et al. (1999), compared the Al Kufrah Basin to pull apart basins in Oman and Saudi Arabia, and suggested that the Najd fault system may extend north into the Al Kufrah Basin and be reactivated as a rift during the Precambrian. Seismic lines of the south of the Al Kufrah Basin do indeed have features which have been interpreted as rifts. However, they are only found in a small area of the basin and the synrift subsidence accounts for a sixth of the overall subsidence (Ghanoush and Abubaker, 2007). The Ghadames Basin has very similar stratigraphy to Al Kufrah, but shows no evidence of rifting. Rifting is not widespread or large enough to cause the subsidence across all the Palaeozoic basins in North Africa. This also means that orogenic collapse is an unlikely subsidence mechanism, given that this is a special case of rifting on thickened continental crust. Armitage and Allen (2010) suggest that these basins can still form due to extension, but when stretching is occurring at low strain rates the strain might not localise along faults. It is hard to distinguish between their model and the model proposed in this paper on the grounds of rifting. Subsidence due to extension at low strain rates produces a period of constant subsidence during stretching followed by decreasing subsidence during the thermal sag phase. Whereas cooling of a thin lithosphere produces subsidence which decreases smoothly throughout time. The latter model fits the backstripping results (Fig. 4) which do not have a kink, but are be closer to a smooth curve.

There are problems with using dynamic topography to explain the basins: it has a transient effect and will rebound once the down welling has ceased leading to uplift and erosion. Nor is it possible at present to model whether the basins in North Africa would have been affected by mantle down-welling during the Palaeozoic. Thermal subsidence on the other hand explains the lateral extent of the subsidence as the lithosphere would be thin across most, if not all, of the

1
2
3
4 553 accretionary crust. Our results show that it is long lasting, fits the magnitude of the observed
5
6 554 subsidence and is able to cause subsidence over a wide range of terranes.

7
8
9 555 Thermal subsidence has a number of important implications. It suggests that one of the
10
11 556 fundamental properties of accretionary crust is that, in the absence of other competing tectonic
12
13
14 557 forces, it will subside after its formation. This will alter the overall composition of the crust,
15
16 558 adding several kilometres of sediments to crust made up largely of island arc and oceanic
17
18
19 559 material. It also predicts that the lithosphere beneath accretionary crust is not depleted by the
20
21 560 melting events which produced the crust, but is compositionally no different to upper mantle.
22
23
24 561 This will make the lithosphere more susceptible to thermal erosion as it does not have
25
26 562 compositional buoyancy and also affect the character of melts originating in it or passing
27
28
29 563 through it. Ashwal and Burke (1989) also noted that this fits the geophysical measurements of
30
31 564 the thickness and seismic properties of the lithosphere and with the geochemistry of Cenozoic
32
33 565 volcanism in North Africa.

34
35
36 566

37 38 567 **6. Conclusions**

39
40
41 568
42
43 569 We have shown that results from backstripping wells in two North African basins and
44
45 570 numerical modelling, are consistent with a basin forming mechanism of lithospheric cooling and
46
47
48 571 thickening, underneath relatively juvenile, accretionary crust. The backstripping revealed that
49
50
51 572 the Ghadames and Al Kufrah basins have experienced their highest rates of subsidence, (22.2
52
53 573 m/Myr and 10.1 m/Myr, respectively) at the start of the Palaeozoic, declining to almost zero at
54
55 574 the end of the Palaeozoic. There is almost no tectonic subsidence during the Mesozoic and
56
57
58 575 Cenozoic. The forward modelling shows that thermal subsidence of accretionary crust provides

1
2
3
4 576 a viable explanation for the formation of the Palaeozoic basins of North Africa, fitting the
5
6
7 577 available data better than previously suggested mechanisms.

8
9 578 We suggest that thermal subsidence following accretion would be expected in other areas of
10
11 579 accretionary crust, and could have influenced the rifted West Siberian Basin. It also predicts that
12
13
14 580 accretionary crust is underlain by fertile mantle lithosphere which may explain why Cenozoic
15
16 581 volcanism in North Africa and Arabia seems to originate from a fertile source (Ashwal and
17
18
19 582 Burke, 1989).

20
21 583
22 584 **Acknowledgements**

23
24
25 585 We thank Statoil for providing funding and well log data for the Ghadames Basin as well as
26
27 586 giving feedback and facilitating discussion with other researchers. We thank Philip Allen and an
28
29
30 587 anonymous reviewer for helpfully pointing out how the paper could be improved and focused.
31
32 588 We also thank Paul Ryan for his advice and input in early stages of the forward modelling.

33
34
35 589
36
37 590 **References**

- 38 591 Abadi, A.M., van Wees, J.-D., van Dijk, P.M., Cloetingh, S.A.P.L., 2008, Tectonics and
39 592 subsidence evolution of the Sirt Basin, Libya. AAPG Bulletin, 92, p. 993-1027.
40
41 593 Abdelsalam, M.G., Liégeois, J.P., Stern, R.J., 2002, The Saharan Metacraton, in: Fritz, H.,
42 594 Loizenbauer, J. (Eds.), 18th colloquium of African Geology J. of African Earth Sci. Graz
43 595 Austria, Elsevier, pp. 119-136.
44 596 Allen, P., Armitage, J.J., in press, Cratonic Basins, in: Busby, C.J., and Ingersoll, R.V. (Eds.),
45 597 Tectonics of sedimentary basins. Cambridge, Blackwell Science.
46
47 598 Allen, P.A., Allen, J., 2005, Basin Analysis. Principles and Applications. Oxford, Blackwell
48 599 Publishing.
49 600 Arcay, D., Doin, M.-P., Tric, E., Bousquet, R., de Capitani, C., 2006, Overriding plate thinning
50 601 in subduction zones: Localised convection induced by slab dehydration. *Geochem.*
51 602 *Geophys. Geosyst.*, 7, p. 26.
52
53 603 Armitage, J.J., Allen, P.A., 2010, Cratonic basins and the long-term subsidence history of
54 604 continental interiors: *J. of the Geol. Soc. of London*, 167, p. 61-70.
55 605 Artyushukov, E.V., 2005, The formation mechanism of the Barents Basin. *Russian Geology and*
56 606 *Geophysics*, 47, p. 683-696.
57
58 607 Ashwal, L.D., Burke, K., 1989, African lithospheric structure, volcanism and topography. *Earth*
59 608 *and Planetary Sci. Lett.*, 96, p. 8-14.

1
2
3
4
5
6
7
8
9
10
11
12
13
14
15
16
17
18
19
20
21
22
23
24
25
26
27
28
29
30
31
32
33
34
35
36
37
38
39
40
41
42
43
44
45
46
47
48
49
50
51
52
53
54
55
56
57
58
59
60
61
62
63
64
65

Bellini, E., Massa, D., 1980, A Stratigraphic contribution to the Paleozoic of the southern basins of Libya, in: Salem, M.J., Busrewil, M.T. (Eds.), The Geology of Libya, 2nd Symposium of the Geology of Libya, Volume 1. Amsterdam, Elsevier, p. 3-56.

Black, R., Latouche, L., Liégeois, J.P., Caby, R., Bertrand, J.M., 1993, Pan African displaced terranes in the Tuareg Shield (central Sahara). *Geology* 22, p. 641-644.

Boote, D.R.D., Clark-Lowes, D.D., Traut, M.W., 1998, Palaeozoic petroleum systems of North Africa, in: MacGregor, D.S., Moody, R.T.J., Clark-Lowes, D.D. (Eds.), *Petroleum Geology of North Africa: London, The Geological Society of London Special Publications No. 132*, p. 7-68.

Brunet, M.-F., Cloetingh, S.A.P.L., 2003, Integrated Peri-Tethyan basins studies (Peri-Tethys programme). *Sedimentary Geology*, 156, p. 1-10.

Bumby, A.J., Guiraud, R., 2005, The geodynamic setting of the Phanerozoic basins of North Africa: *J. of African Earth Sci.*, 43, p. 1-12.

Caby, R., 2003, Terrane assembly and geodynamic evolution of central-western Hoggar: a synthesis. *J. of African Earth Sci.*, 37, p. 133-159.

Capitanio, F.A., Faccenna, C., Funicello, R., 2009, The opening of the Sirte basin: Result of slab avalanching?. *Earth and Planetary Sci. Lett.*, 285, p. 210-216.

Christensen, N.I., Mooney, W.D., 1995, Seismic velocity structure and composition of the continental crust; a global view. *J. of Geophys. Res.*, 100, p. 9761-9788.

Cook, H.E., Zhemchuzhnikov, V.G., Buvtyshkin, V.M., Golub, L.Y., Gatovsky, Y.A., Zorin, Y.A., 1994, Devonian and Carboniferous passive-margin carbonate platform of southern Kazakhstan: Summary of depositional and stratigraphic models to assist in the exploration and production of coeval giant carbonate platform oil and gas fields in the north Caspian Basin, western Kazakhstan., in: Embry, A.F., Beauchamp, B., Glass, G.J. (Eds.), *Pangea: Global Environments and Resources*, Canadian Society of Petroleum Geologists Memoir 17, p. 363-381.

Craig, J., Rizzi, C., Said, F., Thusu, B., Lüning, S., Asbali, A.I., Keeley, M.L., Bell, J.F., Durham, M.J., Eales, M.H., Beswetherick, S., Hamblett, C., in press, Structural Styles and Prospectivity in the Precambrian and Paleozoic Hydrocarbon Systems of North Africa, *Geology of East Libya Symposium 2004*. Binghazi, p. 1-52.

Echikh, K., 1998, Geology and hydrocarbon occurrences in the Ghadames Basin, Algeria, Tunisia, Libya, in: MacGregor, D.S., Moody, R.T.J., Clark-Lowes, D.D. (Eds.), *Petroleum geology of North Africa*, Volume Special Publication No. 132. London, The Geological Society of London Special Publications, p. 109-129.

Elkins Tanton, L.T., Grove, T.L., Donnelly-Nolan, J., 2009, Hot, shallow mantle melting under the Cascades volcanic arc. *Geology*, 29, p. 631-634.

Fekirine, B., Abdallah, H., 1998, Palaeozoic lithofacies correlatives and sequence stratigraphy of the Saharan Platform, Algeria., in: MacGregor, D.S., Moody, R.T.J., Clark-Lowes, D.D. (Eds.), *Petroleum Geology of North Africa*, Volume Special Publications No. 132: London, The Geological Society of London Special Publications, p. 97-108.

Gallagher, K., Demitru, T.A., Gleadow, A.J.W., 1994, Constraints on the vertical motion of eastern Australia during the Mesozoic. *Basin Res.*, 6, p. 77-94.

Gao, S., Luo, T.-C., Zhang, B.-R., Zhang, H.-F., Han, Y.-w., Zhao, Z.-D., Hu, Y.-K., 1998, Chemical composition of the continental crust as revealed by studies in East China. *Geochimica et Cosmochimica Acta*, 62, p. 1959-1975.

1
2
3
4
5
6
7
8
9
10
11
12
13
14
15
16
17
18
19
20
21
22
23
24
25
26
27
28
29
30
31
32
33
34
35
36
37
38
39
40
41
42
43
44
45
46
47
48
49
50
51
52
53
54
55
56
57
58
59
60
61
62
63
64
65

Ghanoush, H., Abubaker, H., 2007, Gravity and Magnetic Profile along Seismic Intersect Ku - 89 - 04, Southern Kufra Basin - Libya, International Conference on Geo-resources in the Middle East and North Africa. Cairo University, Cairo.

Gorbatov, A., Dominguez, J., Suárez, G., Kostoglodov, V., Zhao, D., Gordeev, E., 1999, Tomographic imaging of the *P*-wave velocity structure beneath the Kamchatka peninsula. *Geophys. J. Int.*, 137, p. 269-279.

Grignani, D., Lanzoni, E., Elatrash, H., 1991, Paleozoic and Mesozoic subsurface of palynostratigraphy in the Al Kufra Basin, Libya, in: Salem, M.J., Hammuda, O.S., and Eliagoubi, B.A. (Eds.), *The Geology of Libya*, 3rd symposium of the Geology of Libya, Volume 4, Elsevier, p. 1159-1228.

Guiraud, R., Bosworth, W., 1999, Phanerozoic geodynamic evolution of northeastern Africa and the northwestern Arabian platform: *Tectonophysics*, 315, p. 73-108.

Guiraud, R., Bosworth, W., Thierry, J., Delplanque, A., 2005, Phanerozoic geological evolution of Northern and Central Africa. An overview: *J. of African Earth Sci.*, 43, p. 83-143.

Haq, B.U., Schutter, S.R., 2008, A chronology of Paleozoic sea-level Changes: *Science*, 322, p. 64-68.

Heine, C., Müller, R.D., Steinberger, B., Torsvik, T.H., 2008, Subsidence in intracontinental basins due to dynamic topography. *Physics of the Earth And Planetary Interiors*, 171, p. 252-264.

Holbrook, W.J., Lizarralde, D., McGeary, S., Bangs, N., Diebold, J., 1999, Structure and composition of the Aleutian Island Arc and implications for continental crustal growth. *Geology*, 27, p. 31-34.

Huang, J., Zhong, S., 2005, Sublithospheric small-scale convection and its implications for the residual topography at old ocean basins and the plate model. *J. of Geophys. Res.*, 110 (B8), doi:10.1029/2004JB003153.

Huang, J., Zhong, S., van Hunen, J., 2003, Controls on sublithospheric small-scale convection. *J. of Geophys. Res.*, 108 (B8), doi:10.1029/2003JB002456.

Janssen, M.E., Stephenson, R.A., Cloetingh, S.A.P.L., 1995, Temporal and spatial correlations between changes in plate motions and the evolution of rifted basins in Africa. *Geol. Soc. of America Bull.*, 107, p. 1317-1332.

Kaminski, E., Jaupart, C., 2000, Lithosphere structure beneath the Phanerozoic intracratonic basins of North America. *Earth and Planetary Sci. Lett.*, 178, p. 139-149.

Klein, G.D., 1995, Intracratonic Basins, in: Busby, C.J., Ingersoll, R.V. (Eds.), *Tectonics of Sedimentary basins*. Oxford, England, Blackwell Science, p. 459-478.

Kominz, M., 1995, Thermally subsiding basins and the insulating effect of sediment with application to the Cambro-Ordovician Great Basin sequence, western USA. *Basin Res.*, 7, p. 221-233.

Konert, G., Afifi, A.M., Al-Hajri, S.A., Groot, K.d., Naim, A.A.A., Droste, H.J., 2001, Paleozoic stratigraphy and hydrocarbon habitat of the Arabian Plate, in: Downey, M.W., Threet, J.C., Morgan, W.A. (Eds.), *Petroleum provinces of the twenty-first century*: Tulsa, United States, American Association of Petroleum Geologists, p. 483-515.

Le Heron, D.P., Armstrong, H.A., Wilson, C., Gindre, L., 2010, Glaciation and deglaciation of the Libyan Desert; the Later Ordovician record. *Sedimentary Geology*, 223, p. 100-125.

Lüning, S., Craig, J., Fitches, B., Mayouf, J., Busrewil, A., El Dieb, M., Gammudi, A., Loydell, D., McIlroy, D., 1999, Re-evaluation of the petroleum potential of the Kufra Basin (SE

1
2
3
4
5
6
7
8
9
10
11
12
13
14
15
16
17
18
19
20
21
22
23
24
25
26
27
28
29
30
31
32
33
34
35
36
37
38
39
40
41
42
43
44
45
46
47
48
49
50
51
52
53
54
55
56
57
58
59
60
61
62
63
64
65

699 Libya, NE Chad): does the source rock barrier fall?. *Marine and Petroleum Geology*, 16,
700 p. 693-718.

701 Macpherson, C.G., 2008, Lithosphere erosion and crustal growth in subduction zones: insights
702 from initiation of the nascent East Philippine Arc. *Geology*, 36, p. 311-314.

703 McKenzie, D., 1978, Some remarks on the development of sedimentary basins. *Earth and*
704 *Planetary Sci. Lett.*, 40, p. 25-32.

705 McKenzie, D., Jackson, J., Priestley, K., 2005, Thermal structure of oceanic and continental
706 lithosphere. *Earth and Planetary Sci. Lett.*, 233, p. 337-349.

707 Murphy, J.B., Nance, R.D., 1991, Supercontinent model for the contrasting character of late
708 Proterozoic orogenic belts *Geology*, 19, p. 469-472.

709 Natal'in, B.A., Şengör, A.M.C., 2005, Late Palaeozoic to Triassic evolution of the Turan and
710 Scythian platforms; the pre-history of the palaeo-Tethyan closure. *Tectonophysics*, 404,
711 p. 175-202.

712 Paquette, J.L., Caby, R., Djouadi, M.T., Bouchez, J.L., 1998, U-Pb dating of the end Pan-
713 African orogeny in the Tuareg shield: the post-collisional syn-shear Tiouetine pluton
714 (Western Hoggar, Algeria). *Lithos*, 45, p. 245-253.

715 Parsons, B., Sclater, J.G., 1977, An analysis of the variation of of the ocean floor bathymetry
716 and heat flow with age. *J. of Geophys. Res.*, 108, p. 803-827.

717 Pasyanos, M.E., Nyblade, A.A., 2007, A top to bottom lithospheric study of Africa and Arabia.
718 *Tectonophysics*, 444, p. 27-44.

719 Priestley, K., McKenzie, D., 2006, The thermal structure of the lithosphere from shear wave
720 velocities. *Earth and Planetary Sci. Lett.*, 244, p. 285-301.

721 Richter, F.M., Parsons, B., 1975, On the interaction of two scales of convection in the mantle. *J.*
722 *of Geophys. Res.*, 80, p. 2529-2541.

723 Ritzmann, O., Faleide, J.I., 2009, The crust and mantle lithosphere in the Barents Sea/Kara Sea
724 region. *Tectonophysics*, 470, p. 89-104.

725 Sclater, J.G., Christie, P.A.F., 1980, Continental stretching; an explanation of the post-Mid-
726 Cretaceous subsidence of the central North Sea basin. *J. of Geophys. Res.*, 85, p. 3711-
727 3739.

728 Seber, D., Sandvol, E., Sandvol, C., Brindisi, C., Barazangi, M., 2001, Crustal model for the
729 Middle East and North Africa region: implications for the isostatic compensation
730 mechanism. *Geophys. J. Int.*, 147, p. 630-638.

731 Selley, R.C., 1997, The basins of Northwest Africa; structural evolution, in: Selley, R.C. (Ed.),
732 *African basins: Sedimentary basins of the world: Amsterdam, Elsevier*, p. 17-26.

733 Şengör, A.M.C., Natal'in, B.A., Burtman, V.S., 1993, Evolution of the Altaid tectonic collage
734 and Palaeozoic crustal growth in Eurasia. *Nature*, 364, p. 299-307.

735 Şengör, A.M.C., Okurogullari, A.H., 1991, The role of accretionary wedges in the growth of
736 continents: Asiatic examples from Argand to Plate Tectonics. *Eclogae Geologicae*
737 *Helveticae*, 84, p. 535-597.

738 Shaw, D.M., Cramer, J.J., Higgins, M.D., Truscott, M.G., 1986, Composition of the Canadian
739 Precambrian shield and the continental crust of the earth, in: Dawson, J.B., Carson, D.A.,
740 Hall, J., Wedepohl, K.H. (Eds.), *The Nature of the Lower Continental Crust, Volume 24:*
741 *London, Geological Society of London Special Publications*, p. 275-282.

742 Stampfli, G.M., Borel, G.D., 2002, A plate tectonic model for the Paleozoic and Mesozoic
743 constrained by dynamic plate boundaries and restored synthetic oceanic isochrons. *Earth*
744 *and Planetary Sci. Lett.*, 196, p. 17-33.

- 1
2
3
4 745 Stein, C.A., Stein, S., 1992, A model for the global variation in oceanic depth and heat flow
5 746 with lithospheric age. *Nature*, 359, p. 123-129.
6
7 747 Stern, R.J., 1994, Arc assembly and continental collision in the Neoproterozoic East African
8 748 orogen: Implications for the consolidation of Gondwanaland. *Ann. Rev. of Earth and*
9 749 *Planetary Sci.*, 22, p. 319-351.
10 750 —, 2002, Subduction zones. *Rev. of Geophys.*, 40, doi:10.1029/2001RG000108
11 751 Sultan, M., Chamberlain, K.R., Bowring, S.A., Arvidson, R.E., Abuzied, H., Kaliouby, B.E.,
12 752 1990, Geochronologic and isotopic evidence for involvement of pre-Pan-African crust in
13 753 the Nubian Shield, Egypt. *Geology*, 18, p. 761-764.
14 754 Takahashi, N., Kodaira, S., Klemperer, S.L., Tatsumi, Y., Kaneda, Y., Suyehiro, K., 2007,
15 755 Crustal structure and evolution of the Mariana intra-oceanic island arc. *Geology*, 35, p.
16 756 203-206.
17
18 757 Turcotte, D.L., Schubert, G., 2002, *Geodynamics*. Cambridge, Cambridge University Press.
19 758 Turner, B.R., 1978, Paleozoic sedimentology of the south eastern part of the Al Kufrah Basin,
20 759 Libya: A model for oil exploration, in: Salem, M.J., Busrewil, M.T. (Eds.), *The Geology*
21 760 *of Libya*, 2nd symposium of the Geology of Libya, Volume 2, p. 351-375.
22
23 761 van Hunen, J., Zhong, S., Shapiro, N.M., Ritzwoller, M.H., 2005, New evidence for dislocation
24 762 creep from 3-D geodynamic modeling of the Pacific upper mantle structure. *Earth and*
25 763 *Planetary Sci. Lett.*, 238, p. 146-155.
26
27 764 van Keken, P.E., 2003, The structure and dynamics of the mantle wedge. *Earth and Planetary*
28 765 *Sci. Lett. Frontiers*, 215, p. 323-338.
29
30 766 Van Wees, J.-D., van Bergen, F., David, P., Nepveu, M., Beekman, F., Cloetingh, S.A.P.L.,
31 767 Bonté, D., 2009, Probabilistic tectonic heat flow modeling for basin maturation:
32 768 Assessment method and applications. *Marine and Petroleum Geology*, 26, p. 536-551.
33
34 769 Wedepohl, K.H., 1995, The composition of the continental crust. *Geochimica et Cosmochimica*
35 770 *Acta*, 59, p. 1217-1232.
36 771 Zhao, D., Hasegawa, A., Kanamori, H., 1994, Deep structure of Japan subduction zone as
37 772 derived from local, regional, and teleseismic events. *J. of Geophys. Res.*, 99, p. 22313-
38 773 22329.
39
40 774 Zor, E., Sandvol, E., Gürbüz, C., Türkelli, N., Seber, D., Barazangi, M., 2003, The Crustal
41 775 structure of the East Anatolian plateau (Turkey) from receiver functions. *Geophys. Res.*
42 776 *Lett.*, 30, p. 8044-8048.
43 777
44 778
45
46
47 779

48 780 **Figure Captions**

- 49
50 781
51
52
53 782 **Fig. 1.** Formation of accretionary crust and subsequent lithospheric thickening and subsidence. a) Assembly of
54 783 accretionary crust from island arcs and other crustal fragments through subduction. b) Newly formed accretionary
55 784 crust with a thinned lithosphere. c) Lithospheric thickening due to cooling causing subsidence.
56
57
58

59 785

1
2
3
4
5
6
7
8
9
10
11
12
13
14
15
16
17
18
19
20
21
22
23
24
25
26
27
28
29
30
31
32
33
34
35
36
37
38
39
40
41
42
43
44
45
46
47
48
49
50
51
52
53
54
55
56
57
58
59
60
61
62
63
64
65

Fig. 2. Present outcrop and sub-Mesozoic subcrop of Palaeozoic sediments across North Africa and Arabia (Boote et al., 1998; Konert et al., 2001). Four wells used to construct the Ghadames composite well are located along the line of the transect shown.

Fig. 3. Stratigraphy of the Ghadames and Al Kufrah basins used for backstripping analysis. The Ghadames composite well is constructed from four wells located along the transect shown in Fig. 2, to give the most complete sedimentary record. The locations of the wells from Al Kufrah are also marked on Fig 2.

Fig. 4. Tectonic subsidence curves for the Ghadames and Al Kufrah basins. The solid lines are the tectonic subsidence and the dotted lines show the subsidence if the stratigraphy is entirely shale or sandstone. This envelope is the maximum possible range of variation in the subsidence possible from varying the proportions of the lithologies.

Fig. 5. The right-hand side shows structure and initial temperature conditions for the numerical forward model. The solid line is the preferred temperature profile while the dashed line indicates the potential temperature. The left hand side shows the best estimates for the material properties for the different layers of crust and mantle from the literature. (Allen and Allen, 2005; Shaw et al., 1986; Turcotte and Schubert, 2002)

Fig. 6. The sensitivity of the forward model to variations **(a)** in the crustal thickness and proportion of lower crust (LC) and upper crust (UC), **(b)** the heat production, **(c)** the plate thickness and **(d)** the potential surface temperature of the mantle adiabat.

Fig. 7. Comparison of the subsidence from backstripping the composite well from the Ghadames Basin with a range of forward model runs. The hypothesised subsidence mechanism fits the observed subsidence well although there is a wide range of subsidence over the possible range of variations in the North African crust as demonstrated by the upper and lower limits.

1
2
3
4
5
6
7
8
9
10
11
12
13
14
15
16
17
18
19
20
21
22
23
24
25
26
27
28
29
30
31
32
33
34
35
36
37
38
39
40
41
42
43
44
45
46
47
48
49
50
51
52
53
54
55
56
57
58
59
60
61
62
63
64
65

813 **Table Captions**

814

815 **Table 1** Compilation of intracratonic basins situated on accretionary crust from around the world. The table shows
816 their locations and the temporal link between the end of the accretion event forming the underlying crust and the
817 beginning of subsidence across the basin as a whole.

*Research Highlights

- Thermal subsidence is viable for forming basins on accretionary crust.
- Accretionary crust starts with a thin lithosphere due to formation by subduction.
- Backstripping curves from North African basins suggest thermal subsidence.
- Forward modelling of thermal subsidence is a good match for the backstripping.
- This may also form basins in South America, Central Asia and Eastern Australia.

1
2
3
4 1 Lithospheric cooling and thickening as a basin forming mechanism

5
6
7 2

8
9
10 3 Peter J. Holt^{a*}, Mark B. Allen^a, Jeroen van Hunen^a and Hans Morten Bjørnseth^b.

11 4
12
13 5 ^a Department of Earth Sciences, Durham University, Science Labs, Durham, U.K., DH1 3LE.

14
15 6 ^b Statoil, Forusbeen 50, N-4035 Stavanger, Norway

16
17 7 *Corresponding author, email: p.j.holt@durham.ac.uk

18
19
20 8

21
22 9 ABSTRACT

23
24
25 10
26
27 11 Widely accepted basin forming mechanisms are limited to flexure of the lithosphere, and
28
29 12 lithospheric stretching followed by cooling and thermal subsidence. Neither of these
30
31 13 mechanisms works for a group of large basins, sometimes known as “intracontinental
32
33 14 sags”. In this paper we investigate cooling and thickening of initially thin lithosphere as a
34
35 15 basin forming mechanism, by a combination of forward modelling and a backstripping
36
37 16 study of two Palaeozoic North African basins: Ghadames and Al Kufrah. These are two
38
39 17 of a family of basins, once unified, which lie over the largely accretionary crust of North
40
41 18 Africa and Arabia. Such accretionary crust tends to be juvenile, consisting of
42
43 19 amalgamated island arcs, accretionary prisms and melanges, and typically has near-
44
45 20 normal crustal thicknesses but initially thin mantle lithosphere. Post-accretion subsidence
46
47 21 is modelled using a plate cooling model similar to cooling models for oceanic
48
49 22 lithosphere. The crustal composition and thickness used in the models are varied around
50
51 23 average values of accretionary crust to represent likely heterogeneity. The model allows
52
53 24 the lithosphere to thicken as it cools and calculates the resulting isostatic subsidence.
54
55
56
57
58
59
60
61
62
63
64
65

1
2
3
4
5
6
7
8
9
10
11
12
13
14
15
16
17
18
19
20
21
22
23
24
25
26
27
28
29
30
31
32
33
34
35
36
37
38
39
40
41
42
43
44
45
46
47
48
49
50
51
52
53
54
55
56
57
58
59
60
61
62
63
64
65

25 Water-loaded tectonic subsidence curves from these forward models are compared to
26 tectonic subsidence curves produced from backstripped wells from Al Kufrah and
27 Ghadames basins. A good match between the subsidence curves for the forward model
28 and backstripping is produced when the best estimates for the crustal structure,
29 composition and the present day thickness of the lithosphere for North Africa are used as
30 inputs for the forward model. The model produces sediment loaded basins of 2-7 km
31 thickness for the various crustal assemblies over ~250 Myrs. This shows that lithospheric
32 cooling provides a viable method for producing large basins with prolonged subsidence,
33 without the need for initial extension, provided the condition of initially thin mantle
34 lithosphere is met.

35
36
37

37 **Keywords: basin, lithosphere, subsidence, North Africa**

38

39 **1. Introduction**

40

41 Conventional basin formation mechanisms can be divided into two categories, lithospheric
42 stretching followed by thermal subsidence proportional to the extension (rift basins) and flexure
43 caused by tectonic loading (foreland basins) (Allen and Allen, 2005). However, there is scant
44 evidence for either of these mechanisms forming a group of basins normally classified as
45 “intracontinental sags” – a term that describes their geometry rather than the process of
46 formation. Examples include the Williston and Michigan basins of North America (Klein,
47 1995), the Palaeozoic basins of North African and Arabia (Boote et al., 1998; Konert et al.,

1
2
3
4
5
6
7
8
9
10
11
12
13
14
15
16
17
18
19
20
21
22
23
24
25
26
27
28
29
30
31
32
33
34
35
36
37
38
39
40
41
42
43
44
45
46
47
48
49
50
51
52
53
54
55
56
57
58
59
60
61
62
63
64
65

48 2001); and the Mesozoic Scythian and Turan platforms (Natal'in and Şengör, 2005). The basins
49 are large features, commonly over 1000 km in length, with remarkably uniform, prolonged,
50 gentle subsidence across them, lasting over 200 Myrs. They generally have a polyphase history
51 with a main subsidence phase either preceded or followed by other periods of subsidence and
52 uplift which modify the basin. Armitage and Allen, (2010) recently proposed that these basins
53 are formed by stretching under low strain rates. They argued this based upon the modelling of
54 rifting under low strain rates and the observation that the initiation of subsidence in many
55 intracontinental basins coincides with supercontinent breakup and therefore a broad extensional
56 regime. However, in many basins the evidence for rifting is poor and a number of other
57 mechanisms have been proposed. Subsidence due to cooling of thermal anomalies in the
58 lithosphere has been proposed for the North American intracontinental basins (Kaminski and
59 Jaupart, 2000). The main evidence for this is matching modelling results with the shape and
60 thickness of the present day sedimentary cover. A density change in the crust due to phase
61 changes such as a basalt underplate changing to eclogite has also been suggested based on high
62 velocities in the lower crust interpreted from seismic refraction data (Artyushukov, 2005).
63 However, beneath the Barents/Kara sea region a high density area in the lower crust, suggested
64 by modelling gravity data, has been deemed too local to cause subsidence across the basin.
65 Instead Ritzmann and Faleide, (2009) have suggested that a deeper high velocity zone visible in
66 seismic tomography is evidence of a thick cratonic lithosphere, which causes the subsidence.
67 Heine et al. (2008) noted that many intracratonic basins overlie areas of mantle which have been
68 down welling over the last 100-150 Myrs in their coupled plate and mantle flow model. They
69 proposed that dynamic topography could form these basins. Other subsidence mechanisms and
70 variations on those above have been suggested and are debated in more detail by Armitage and

1
2
3
4 71 Allen (2010) and Klein (1995). It is likely that one mechanism does not explain the formation of
5
6 72 every intercontinental basin and in some cases the basin may be formed by a combination of
7
8
9 73 mechanisms.

10
11 74 Here we show that cooling and thickening of initially thin mantle lithosphere, beneath crust
12
13
14 75 of normal thickness (~30 km) is a viable mechanism for producing basin-scale subsidence. Such
15
16 76 initial conditions are typical of accretionary crust, a term used to summarise the vast orogenic
17
18
19 77 collages of largely juvenile crust and mantle lithosphere, formed by the collision of non-cratonic
20
21 78 terranes: island arcs, accretionary prisms, ophiolites and isolated microcontinents (Murphy and
22
23
24 79 Nance, 1991; Şengör et al., 1993). This would neatly explain the formation of many of the
25
26 80 intracratonic basins on juvenile continental crust such as the Pan African mobile belt or the
27
28
29 81 Scythian and Turan platform. However, we show that where the lithosphere is thinned by a
30
31 82 thermal anomaly it is also possible to form broad, slowly subsiding basins.

32
33 83 This subsidence mechanism is discussed in greater detail in section 2 below, followed by a
34
35
36 84 case study of two of the North African Palaeozoic basins. Thermal subsidence has been
37
38 85 suggested as the cause of intracratonic basins before (Guiraud et al., 2005; Kaminski and
39
40
41 86 Jaupart, 2000; Kominz, 1995). Our contribution is to model the subsidence, compare it to
42
43 87 subsidence in two case studies and to discuss why the lithosphere is plausibly thin in the first
44
45
46 88 place. The subsidence history of the basins is analysed using backstripping. This analysis is
47
48 89 compared to results from a numerical forward model of thermal subsidence acting on
49
50
51 90 accretionary crust, designed to test if it is a mechanism capable of producing the observed
52
53 91 subsidence.

54
55 92

56
57
58 93 **2. Geological background and hypothesis**

1
2
3
4
5
6
7
8
9
10
11
12
13
14
15
16
17
18
19
20
21
22
23
24
25
26
27
28
29
30
31
32
33
34
35
36
37
38
39
40
41
42
43
44
45
46
47
48
49
50
51
52
53
54
55
56
57
58
59
60
61
62
63
64
65

94

95 Seismic refraction studies show that present day island arcs can have a crustal thickness of
96 25-35 km, similar to normal continental crust (Holbrook et al., 1999; Takahashi et al., 2007).
97 However, seismic tomography shows slow velocities in the mantle wedge below island arcs
98 which are interpreted as evidence for the presence of melts and thin (~20 km) mantle lithosphere
99 because it is weakened by the addition of fluids from the subducting slab and then eroded by the
100 corner flow in the mantle wedge (Gorbatov et al., 1999; Zhao et al., 1994). This is supported by
101 numerical models of subduction (Arcay et al., 2006; Stern, 2002; van Keken, 2003), by
102 geochemical evidence from the southward initiation of the Philippine subduction zone
103 (Macpherson, 2008) and from the Cascades (Elkins Tanton et al., 2009). These studies suggest
104 an average overall lithospheric thickness of about 50 km beneath island arcs (Fig. 1a).

105 Accretionary prisms may be 30 km thick, largely composed of off-scraped and imbricated
106 fragments of oceanic crust and its sedimentary cover. Whilst subduction is active such prisms
107 are underlain by the oceanic plate. When subduction has recycled the oceanic plate in to the
108 mantle, the base of the prism may be in contact with the asthenosphere, particularly if ocean
109 closure resulted in the collision of two such prisms, initially on opposite sides of the ocean,
110 rather than collision of the prism with a continental margin. The Cenozoic East Anatolian
111 Accretionary Complex may be an example of such a lithospheric structure, where tomographic
112 studies suggest a thin or even absent mantle lithosphere (Zor et al., 2003).

113 A notable feature of accretionary orogenic belts is that they lack evidence for substantial
114 crustal thickening (and presumably lithosphere thickening): there is rarely evidence for pre-
115 collision passive continental margins, Alpine-type nappes, or overfilled foreland basins
116 (“molasse”) (Şengör and Okurogullari, 1991). This means that putative lithospheric

1
2
3
4
5
6
7
8
9
10
11
12
13
14
15
16
17
18
19
20
21
22
23
24
25
26
27
28
29
30
31
32
33
34
35
36
37
38
39
40
41
42
43
44
45
46
47
48
49
50
51
52
53
54
55
56
57
58
59
60
61
62
63
64
65

117 delamination following an orogeny of this type, hypothesised by Ashwal and Burke, (1989), is
118 not our preferred mechanism for thinning the lithosphere. However, it would produce similar
119 starting conditions to those in our model.

120 As accretionary crust is assembled through subduction and collision, the thin mantle
121 lithosphere of the original terranes is inherited by the final collage (Fig. 1b). We hypothesise
122 that once accretion is completed, and subduction has ceased beneath an area, the underlying
123 asthenosphere will cool, thickening the mantle lithosphere. This cooling will cause prolonged
124 subsidence, forming basins (Fig. 1c).

125 *Figure 1 should be placed here*

126 Our model is similar to the thermal subsidence phase of McKenzie style rifting (McKenzie,
127 1978) or the subsidence of the ocean floor away from a mid ocean ridge, except that the crust
128 involved is continental, albeit juvenile, and has not been thinned in any way. In this paper we
129 proceed to show how this mechanism could produce the basins in North Africa. However, there
130 are many other intracratonic basins on accreted crust where this mechanism could apply. Table
131 1 provides a sample of some of the basins we aware of, but is by no means an exhaustive list.
132 Allen and Armitage, (in press) note a clustering in time of the initiation of intracratonic basins
133 which they link to the breakup of supercontinents. In Table 1 we show the start of subsidence
134 follows closely the end of accretion and the clustering may be related to the end of periods of
135 accretion of crust. The basins are long lived features and so many have later phases of
136 subsidence which potentially have other causes.

137 *Table 1 should be placed here.*

138

139 **3. Tectonic subsidence history of backstripped North African basins**

1
2
3
4
5
6
7
8
9
10
11
12
13
14
15
16
17
18
19
20
21
22
23
24
25
26
27
28
29
30
31
32
33
34
35
36
37
38
39
40
41
42
43
44
45
46
47
48
49
50
51
52
53
54
55
56
57
58
59
60
61
62
63
64
65

140
141
142
143
144
145
146
147
148
149
150
151

In order to test whether the proposed mechanism of subsidence provides a good explanation for anomalous basins developed over accretionary crust, subsidence histories for the Ghadames and Al Kufrah basins were investigated using backstripping. These are Palaeozoic basins situated on the North African crust, which was accreted in the Pan African orogeny during Neoproterozoic times (Caby, 2003; Stern, 1994). Most of the basement to North Africa and Arabia is juvenile, generated and assembled during the Pan African orogeny. The western margin is the West African Craton. The southern limit is the Congo Craton. The eastern and northern limits are not so well defined because of later rifting and collision with Eurasia. For example, similar basement underlies much of the territory of Iran, but with a more complicated Mesozoic and Cenozoic magmatic and tectonic history. The outcrop or sub-Mesozoic subcrop of the Palaeozoic strata of North Africa and Arabia is shown in Fig. 2.

Figure 2 should be placed here

152
153
154
155
156
157
158
159
160
161
162

The proportion of cratonic nuclei within this vast, 10,000,000 km² orogen is debated, but plausibly is small. There are indications of pre Late Proterozoic crust within North Africa, based on Meso- or Palaeo-Proterozoic isotopic model ages and detrital zircons in younger metamorphic terranes (Black et al., 1993; Sultan et al., 1990). But the Late Proterozoic tectonic overprint is severe, suggesting that extensive magmatic and metamorphic re-working and additions took place during the Pan African orogeny, and no single, regionally extensive block survived the Late Proterozoic orogeny with its original structure and boundaries preserved. A significant re-worked region has been called the Saharan metacraton (Abdelsalam et al., 2002), but this is not recognised by all workers e.g. (Bumby and Guiraud, 2005). Whatever the nature and origins of the Saharan metacraton, it appears to have had little impact on the overlying

1
2
3
4
5
6
7
8
9
10
11
12
13
14
15
16
17
18
19
20
21
22
23
24
25
26
27
28
29
30
31
32
33
34
35
36
37
38
39
40
41
42
43
44
45
46
47
48
49
50
51
52
53
54
55
56
57
58
59
60
61
62
63
64
65

163 Phanerozoic basins (Fig. 2). These are continuous across the metacraton margins, without
164 discernible change in sedimentary thickness or composition.

165 The end of the Pan African orogeny was diachronous. Local timings for the last deformation
166 vary from Late Precambrian to the Early Cambrian e.g. (Paquette et al., 1998). Present-day
167 lithosphere thickness across North Africa is on the order of ~100 km (Pasyanos and Nyblade,
168 2007; Priestley and McKenzie, 2006); except for the West African Craton where it reaches >200
169 km. Crustal thicknesses are not well-constrained, but are variously estimated at 30 to 40 km
170 thick from gravity and seismic interpretations (Seber et al., 2001), or 25 to 35 km from the
171 inversion of surface waves (Pasyanos and Nyblade, 2007).

172 The Ghadames Basin is well studied because large hydrocarbon accumulations have been
173 discovered within it (Echikh, 1998). Several wells have penetrated the crystalline basement and
174 there are large amounts of seismic data for the basin. This means the geometry of the basin is
175 well understood. This allows the most complete stratigraphic sections to be identified, which is
176 helpful when backstripping. The Al Kufrah Basin is less well studied and has only two
177 published wells which reached the crystalline basement (Grignani et al., 1991). To a first order,
178 it has a similar Palaeozoic stratigraphy to the Ghadames Basin. Enough data are available for Al
179 Kufrah to make it viable for modelling.

180

181 *3.1 Methodology*

182

183 Backstripping is a well known technique for calculating the tectonic subsidence of a
184 particular horizon in a basin over time. We use the basement/cover boundary, which reveals the
185 overall subsidence (Allen and Allen, 2005; Sclater and Christie, 1980). The technique first

1
2
3
4
5
6
7
8
9
10
11
12
13
14
15
16
17
18
19
20
21
22
23
24
25
26
27
28
29
30
31
32
33
34
35
36
37
38
39
40
41
42
43
44
45
46
47
48
49
50
51
52
53
54
55
56
57
58
59
60
61
62
63
64
65

186 decompacts each sedimentary layer through time. This gives the total subsidence curve for the
187 basement which is assumed to be composed of the tectonic subsidence, the isostatic effect
188 (weight) of the sediments and the changes in water depth compared to the present day sea level.
189 The effects of the sediments and sea level changes are removed so that the remaining subsidence
190 is due purely to the tectonic driving force. A global eustatic sea-level curve of (Haq and
191 Schutter, 2008) is used to remove the effects of sea-level changes.

192 The backstripping method assumes that the compaction of the sediments is purely
193 mechanical (due to the weight of the sediments above) and ignores chemical processes, such as
194 cementation, which are very difficult to take into account because they depend on a complex
195 series of factors such as fluid flow, composition, temperature and pressure. Backstripping
196 assumes that the sediments are laid down in successive layers throughout time and does not take
197 into account periods of uplift and erosion or non deposition. These are difficult to include in
198 backstripping because generally the amount of eroded material is poorly constrained. If the
199 present day burial depth of the basement is the deepest it has been, then any erosion will make
200 no difference because the sediments are at their peak pressure. Otherwise the compaction of the
201 sediments will be underestimated. There are no porosity depth relationships available for the
202 sediments in North Africa and we use standard relationships from published work (Sclater and
203 Christie, 1980). We assume that the compaction curves, which are based on sediments from the
204 North Sea, are applicable to the sediments in North Africa. This is justifiable because the North
205 African sediments are entirely siliciclastic and are similar to those in the North Sea.

206 This method was applied to a composite well from the Ghadames Basin. A composite well
207 was used because it gives the most complete section possible from the basin therefore showing
208 the maximum subsidence and limiting the effect of erosion. The composite well was created

1
2
3
4
5
6
7
8
9
10
11
12
13
14
15
16
17
18
19
20
21
22
23
24
25
26
27
28
29
30
31
32
33
34
35
36
37
38
39
40
41
42
43
44
45
46
47
48
49
50
51
52
53
54
55
56
57
58
59
60
61
62
63
64
65

209 using four unpublished wells from the transect shown on Fig. 2, to identify the most complete
210 sections and to ensure that the differences in the thickness of the layers were due to variations in
211 erosion rather than deposition rates. This minimises the errors related to eroded sections of the
212 stratigraphy. It also produces a subsidence curve which emphasises the subsidence phases rather
213 than any uplift. This allows us to see clearly the main subsidence phase associated with basin
214 formation, rather than later phases of uplift or subsidence. This approach was not possible in the
215 Al Kufrah Basin because of the scarcity of available well data, and instead the backstripping
216 methodology was applied directly to the two available wells.

217

218 *3.2 General Stratigraphy*

219

220 Detailed descriptions of the stratigraphy in the Ghadames, Al Kufrah and other North African
221 basins can be found in papers such as Bellini and Massa (1980), Echikh (1998), Fekirine and
222 Abdallah (1998), Grignani et al. (1991) and Lüning et al. (1999). Therefore we present a brief
223 summary of the evolution of the Palaeozoic basins on the accretionary crust of North Africa
224 collated from Boote et al. (1998), Bumby and Guiraud (2005), Craig et al. (in press), Guiraud
225 and Bosworth (1999) and Guiraud et al. (2005) alongside more detailed observations from the
226 basins themselves. The basins are filled with a largely siliciclastic succession with some
227 evaporites and carbonates towards the end of the Palaeozoic. The whole of North Africa
228 subsided as a large platform from roughly the start of the Palaeozoic, depositing a wedge of
229 sediments that thinned to the south (Selley, 1997). Only localised Late Proterozoic/Early
230 Palaeozoic rifting is known (see Fig. 6 of Guiraud et al. (2005), and as several of the main
231 basins are mature in terms of hydrocarbon exploration it is unlikely that major rifts have been

1
2
3
4
5
6
7
8
9
10
11
12
13
14
15
16
17
18
19
20
21
22
23
24
25
26
27
28
29
30
31
32
33
34
35
36
37
38
39
40
41
42
43
44
45
46
47
48
49
50
51
52
53
54
55
56
57
58
59
60
61
62
63
64
65

missed. Seismic lines through the Kufrah Basin show Late Proterozoic/Cambrian rifts (Lüning et al., 1999), however these are only seen on seismic lines in the south of the basin (Ghanoush and Abubaker, 2007) and do not explain subsidence across the whole basin or in neighbouring basins. Nor do the dimensions of the subsiding area ($\gg 1000$ km) fit a flexural, foreland basin mechanism. In any case, there is no record of an appropriate orogeny lasting through the Palaeozoic along the Gondwanan continental margin (Stampfli and Borel, 2002). The initial sediments are largely fluvial sandstones and conglomerates in the Cambrian, changing to marine sandstones in the early Ordovician. The Cambrian age for the earlier sediments is inferred because there are very few trace fossils to date the sediments until the marine incursions (Grignani et al., 1991). In the mid to late Ordovician there was major glaciation creating a regional erosional surface (Le Heron et al., 2010). The amount of erosion varies greatly reflecting the geometry of the ice sheets. Locally in Al Kufrah the erosion cuts down to the Cambrian, but in other areas a complete section to the Mid Silurian is preserved. In these areas the erosion is minimal and the glaciation reflects a period of non deposition. The erosion becomes less severe to the north into the Murzuq and Ghadames basins (Bellini and Massa, 1980; Fekirine and Abdallah, 1998).

Coarse to medium grained sandstones and tillites related to the retreat of the glaciers were deposited at the end of the Ordovician. This was followed by a major marine transgression leading to the deposition of shales throughout the Early Silurian, but water depths decreased with time and the shales grade up to shoreface sandstones. The shales at the base of the Silurian are one of the main source rocks and record the maximum water depth experienced by the basins during the Palaeozoic. Turner (1978) interpreted it as a shallow shelf environment with water depths of about 200 m. Separation of individual basins began during the Silurian caused

1
2
3
4
5
6
7
8
9
10
11
12
13
14
15
16
17
18
19
20
21
22
23
24
25
26
27
28
29
30
31
32
33
34
35
36
37
38
39
40
41
42
43
44
45
46
47
48
49
50
51
52
53
54
55
56
57
58
59
60
61
62
63
64
65

255 by a period of compression most likely related to the Acadian collision (Guiraud and Bosworth,
256 1999). This resulted in an unconformity across the basins of North Africa, but within basins it is
257 localised over arches, such as uplift of the arch between the Ghadames and Murzuq basins
258 (Boote et al., 1998). During the Devonian the basins were filled with shallow marine sandstones
259 and siltstones, and fluvial sandstones, corresponding to fluctuations in sea-level. The
260 transgressions and regressions, as well as prograding systems, can be correlated between basins
261 (Bellini and Massa, 1980). The southern basins (i.e. Al Kufrah) show a greater continental
262 influence compared with the basins further to the north (i.e. Ghadames) (Boote et al., 1998).

263 Deposition at the start of the Carboniferous was similar to the Devonian, with variations in
264 siliciclastic sediments controlled by sea-level changes, but with some carbonates deposited
265 locally in the Ghadames Basin (Fekirine and Abdallah, 1998). The Palaeozoic sediments were
266 terminated by the Late Carboniferous-Permian Hercynian orogeny, which was an important
267 period of compression, causing uplift along the flanks of many of the basins and forming much
268 of the Palaeozoic subcrop pattern seen in Fig 2. In some areas, such as beneath the Sirte Basin, it
269 eroded down to the Cambrian sediments (Abadi et al., 2008). Mesozoic and Cenozoic tectonics
270 related to the opening and closing of Tethys to the north of North Africa, and the opening of the
271 Atlantic Ocean, modified some of the basin geometries and subsidence patterns. The Sirte Basin
272 began forming as a rift basin during the late Cretaceous (100-70 Myrs), and continued to the
273 Early Eocene. Extension was due to far-field stresses related to changes in the spreading rate of
274 the Central and South Atlantic (Guiraud et al., 2005; Janssen et al., 1995). However, this has
275 recently been challenged by Capitano et al. (2009) who suggest this does not fit the timing of
276 extension, and that a better explanation is that the African plate was placed under tensile stress
277 by avalanching of its subducted northern edge through the 660 km discontinuity, beneath the

1
2
3
4
5
6
7
8
9
10
11
12
13
14
15
16
17
18
19
20
21
22
23
24
25
26
27
28
29
30
31
32
33
34
35
36
37
38
39
40
41
42
43
44
45
46
47
48
49
50
51
52
53
54
55
56
57
58
59
60
61
62
63
64
65

278 Hellenic arc. This basin borders the Murzuq and Al Kufrah basins, but was formed later, and so
279 is not analogous to the basins specifically considered in this study. There is little evidence of
280 similar extension in the surrounding basins at this period as shown by the thickness of the
281 Cretaceous deposits seen in the wells from Fig. 4. Similar Palaeozoic successions are seen in the
282 Reggane, Ahnet and Tindouf basins to the north of the West African Craton (Boote et al., 1998).
283 The major event affecting the Paleozoic basins is the Alpine unconformity caused by uplift
284 related to collision of Africa and Europe at the end of the Eocene. See Brunet and Cloetingh
285 (2003) and papers therein for descriptions of the Carboniferous-Recent evolution of basins
286 within northern North Africa and Arabia. These events uplifted the basin margins, and in some
287 areas obscured the earlier subsidence by removing significant thicknesses of sediments. Much of
288 the erosion is focused on the flanks of the basins, although some does occur within the basins, as
289 evidenced by missing Carboniferous section in the well A1 from Al Kufrah (Fig 3). We have
290 sought to minimise the effects of erosion as outlined in our methodology. Details of the
291 stratigraphy for the three wells which were backstripped are shown in Fig. 3.

292 *Figure 3 should be placed here*

294 3.3 Results

296 Fig. 4 shows the tectonic subsidence profiles derived from the backstripping. The profiles
297 start at the beginning of the Cambrian, but the precise time of the onset of subsidence is poorly
298 constrained because the sediments are fluvial sandstones, with no fossils. The subsidence rates
299 are fairly rapid to begin with and slow gradually through time with little or no tectonic
300 subsidence during the Mesozoic and Cenozoic (fastest rates are 22.2 m/Myr in Ghadames and

1
2
3
4
5
6
7
8
9
10
11
12
13
14
15
16
17
18
19
20
21
22
23
24
25
26
27
28
29
30
31
32
33
34
35
36
37
38
39
40
41
42
43
44
45
46
47
48
49
50
51
52
53
54
55
56
57
58
59
60
61
62
63
64
65

301 10.1 m/Myr in Al Kufrah). The subsidence profiles are steadily decaying curves without clearly
302 separate rift and thermal subsidence phases, i.e. they resemble the thermal subsidence that
303 typically follows rifting, without a rift phase being apparent. The subsidence curves show very
304 little tectonic subsidence affected the basins after 250 Myrs, showing that later periods of
305 subsidence, such as that in the Sirte basin, only slightly modified the Ghadames and Al Kufrah
306 basins. The tectonic subsidence is not smooth; the curves show the periods of erosion and uplift
307 evident in the sedimentary record, e.g. Late Palaeozoic, Hercynian, uplift.

308 *Figure 4 should be placed here*

309 Both basins show very similar tectonic subsidence patterns, both in the timing and the
310 amount of the tectonic subsidence. This is evidence that one causal mechanism generated the
311 Palaeozoic subsidence across North Africa. The total tectonic subsidence in the Ghadames
312 composite well is ~2230 m. This is similar to the ~1740 m of subsidence calculated for the
313 B1NC43 well in the Al Kufrah Basin. As Fig. 4 shows, well A1NC43 appears to have had less
314 subsidence (~1260 m). However much of the Carboniferous stratigraphy has been removed by
315 the Hercynian deformation, so this lower total is plausibly an effect of erosion rather than
316 differential subsidence.

317 The uncertainties involved come from the input parameters and the assumptions. These
318 include the thickness and depths of the sedimentary layers from errors in picking horizons from
319 well logs or due to erosion. Estimates of these are not provided by Grignani et al. (1991).
320 Assuming that compaction is entirely mechanical also introduces uncertainties. The errors from
321 using the general compaction curves were estimated by carrying out the backstripping with the
322 entire sedimentary column being made of either shale or sandstones which form the two end
323 members of the compaction curves (Sclater and Christie, 1980). Depositional water depth can

1
2
3
4
5
6
7
8
9
10
11
12
13
14
15
16
17
18
19
20
21
22
23
24
25
26
27
28
29
30
31
32
33
34
35
36
37
38
39
40
41
42
43
44
45
46
47
48
49
50
51
52
53
54
55
56
57
58
59
60
61
62
63
64
65

324 contribute to large uncertainties because it is difficult to tell the depth of sediments deposited in
325 deep water. As shown in section 3.2, in the basins in North Africa this is not such an issue
326 because all sediments were deposited in shallow waters less than 200 m (Grignani et al., 1991).
327 The uncertainties in water depth estimates for shallow water sediments are much smaller (10s of
328 meters). There are also errors related to corrections for the eustatic sea-level. The largest sea-
329 level fluctuations do not exceed 200 m, so the uncertainties in water depths and eustatic sea-
330 level will have little effect on the overall shape of the curves. The errors from the backstripping
331 calculations are shown as the dashed lines in Fig. 4. The errors make a negligible difference to
332 both the shape of the curves and the overall amount of subsidence.

333

334 **4. Forward Modelling**

335

336 Numerical forward modelling of basement subsidence was used to test whether lithospheric
337 cooling and growth is a realistic mechanism for the subsidence of accretionary crust. This is
338 compared to the backstripped results from basins in North Africa to determine if it fits the
339 observed subsidence. The modelling was carried out using Matlab and the code was tested
340 against analytical solutions.

341

342 *4.1 Methodology of the forward modelling*

343

344 The numerical subsidence model is based on and tested against the plate models for sea floor
345 spreading (Parsons and Sclater, 1977; Stein and Stein, 1992). It is modified to include layered
346 continental crust with radioactive heat production. It solves the vertical conductive heat flow

1
2
3
4
5
6
7
8
9
10
11
12
13
14
15
16
17
18
19
20
21
22
23
24
25
26
27
28
29
30
31
32
33
34
35
36
37
38
39
40
41
42
43
44
45
46
47
48
49
50
51
52
53
54
55
56
57
58
59
60
61
62
63
64
65

347 through a one-dimensional column of the lithosphere and upper mantle.

$$348 \quad \rho C_p \frac{\partial T}{\partial t} = \frac{\partial}{\partial z} \left(k \frac{\partial T}{\partial z} \right) + A \quad (1)$$

349 Equation 1 is solved using a finite difference technique with a grid resolution of 1 km. T is
350 the temperature of the rock at a particular point in the grid at depth z . A is the contribution of
351 radioactive heat production and t is the time over which the temperature is changing. Time-
352 stepping is performed with an Euler forward time-integration scheme. The material properties of
353 the rock are the thermal conductivity (k), the specific heat capacity (C_p) and the density (ρ). The
354 density of the rock is dependant on the temperature and is calculated using equation 2.

$$355 \quad \rho = \rho_0 (1 - \alpha(T - T_0)) \quad (2)$$

356 In equation 2 the reference density (ρ_0) and the coefficient of thermal expansion (α) are
357 dependant on the rock type (Turcotte and Schubert, 2002). The values used for all the
358 parameters in equations 1 and 2 are shown in Fig. 5.

359 *Figure 5 should be placed here*

360 The model is set up with a two layer crust composed of a felsic upper crust and granulitic
361 lower crust which is underlain by mantle lithosphere. The base of the lithosphere is purely
362 thermal rather than compositional and describes the temperature below which the mantle rock
363 does not deform significantly over geological timescales. The 1200 °C isotherm is used
364 (Turcotte and Schubert, 2002). The model starts with a 20 km thick mantle lithosphere, which
365 matches the starting conditions described in section 2. The temperature at the surface of the
366 model is set as 0°C. The temperature at the base of the model is calculated using a potential
367 temperature at the surface using an adiabatic gradient of 0.3°C per km. Constant temperature
368 boundary conditions are used at the top and bottom of the model. The initial temperature
369 conditions follow the mantle adiabat to up to a transition point 20 km below the crust above

1
2
3
4
5
6
7
8
9
10
11
12
13
14
15
16
17
18
19
20
21
22
23
24
25
26
27
28
29
30
31
32
33
34
35
36
37
38
39
40
41
42
43
44
45
46
47
48
49
50
51
52
53
54
55
56
57
58
59
60
61
62
63
64
65

370 which they follow a linear gradient to the surface. The depth and therefore temperature at this
371 transition point is dependent on the thickness of the crust and the potential temperature for the
372 surface. The initial conditions for the model are shown in Fig. 5. The temperature profile is used
373 to calculate the density at grid point in the column from the reference density using equation 2.
374 The elevation is calibrated from the density profile of the column using a column of hot mid
375 ocean ridge material with a 7 km thick basaltic-gabbroic crust at 3 km below sea-level as
376 reference. Standard Pratt isostasy (Allen and Allen, 2005) is used. When the topography of the
377 model drops below sea level the basin is filled with water. The thermal boundary condition is
378 applied to the basement floor because water in the basin would have an almost uniform
379 temperature due to convection. However, the water is included in the isostasy so the model
380 effectively produces water loaded tectonic subsidence.

381 One inherent weakness of the plate model is that it only calculates the heat transfer by
382 conduction (Parsons and Sclater, 1977). At the base of the plate heat transfer changes from
383 conduction to convection (Huang et al., 2003; Richter and Parsons, 1975; van Hunen et al.,
384 2005). The plate model does not explicitly describe the physics of this transition, but provides a
385 very good fit to the bathymetry and heatflow data (Huang and Zhong, 2005) and included
386 references. It does not help explain the physical process that causes the thermal boundary layer
387 to become stable at this depth. We ignore the temperature dependence of k , C_p and α . This
388 assumption slightly overestimates temperatures in the top half of the model and underestimates
389 temperatures in the bottom half of the model (McKenzie et al., 2005). This means the depth to
390 the base of the lithosphere is an upper limit.

391

392 *4.2 Results: Effects of varying parameters and the best fit model for the backstripping*

1
2
3
4
5
6
7
8
9
10
11
12
13
14
15
16
17
18
19
20
21
22
23
24
25
26
27
28
29
30
31
32
33
34
35
36
37
38
39
40
41
42
43
44
45
46
47
48
49
50
51
52
53
54
55
56
57
58
59
60
61
62
63
64
65

393

The model is set up so that the each of the parameters from equation 1 can be changed and the structure of the model, shown in Fig. 5, can be altered. Changing these will alter the subsidence produced. It is important to understand how these different parameters affect the subsidence before trying to find the best fitting model because there may be a trade off between different parameters.

399

The model is most sensitive to changes in the thickness of the crust and the plate thickness because they change the isostasy by varying the amount of low density crust and high density lithosphere. However, changing the plate thickness affects the timing of the subsidence whereas changing the crustal thickness only affects the total subsidence so their effects can be distinguished. There is not a direct trade-off between the two parameters. The model is less sensitive to variations in the potential temperature and radioactive heat production respectively (Fig. 6). In each case only the parameter under investigation is changed and the estimates for North African crust shown in Fig. 5 are used as the default the parameters. The amount of variation in the input parameters is based on the uncertainties and variation across North Africa from the literature. The present day thickness of the crust of North Africa was calculated to be between 30 and 40 km thick from low resolution gravity and seismic interpretations and gravity modelling in the 3-D crustal model of Seber et al. (2001) over the area of interest. This is thicker than the crustal thickness of 25-35 km estimated from the inversion of surface waves given by Pasyanos and Nyblade (2007). Due to the uncertainty in crustal thickness our model calculations were run for a range of crustal assemblages between 20 and 40 km thick. The results are shown in Fig. 6a. With a crustal thickness of 40 km, ~ 1.2 km of tectonic subsidence takes place, however the crust is too buoyant to drop below sea-level, so no basin is formed. When the crust

1
2
3
4
5
6
7
8
9
10
11
12
13
14
15
16
17
18
19
20
21
22
23
24
25
26
27
28
29
30
31
32
33
34
35
36
37
38
39
40
41
42
43
44
45
46
47
48
49
50
51
52
53
54
55
56
57
58
59
60
61
62
63
64
65

416 is reduced to 36 km thick the total subsidence increases to ~1.9 km and 1 km of water loaded
417 tectonic subsidence is recorded. A 20 km thick crust starts at 1.4 km below sea-level and
418 experiences ~2.7 km of tectonic subsidence as the lithosphere cools and thickens. There have
419 been no deep crustal seismic lines of North Africa published so the proportion of upper crust
420 and lower crust is unknown. Therefore the model was run with a 30 km thick crust where the
421 thickness of the upper crust was varied between 10 and 20 km. This alters the total subsidence
422 by about 500 m. A 1 km decrease in the total crustal thickness causes ~150 m of additional
423 subsidence, whereas changing 1 km of upper crust to lower crust only increases the total
424 subsidence by ~ 50 m. The main reason both these parameters affect the overall subsidence is
425 that they change the isostasy by varying the amount of low density crust. In all these scenarios
426 the timing of the subsidence does not change, most of the subsidence occurs in the first 100
427 Myrs and the subsidence after 200 Myrs is negligible.

Figure 6 should be placed roughly here in the text

429 We also change the amount of radiogenic heat production. Estimations of heat production in
430 the continental crust vary between 1.31 mWm^{-3} and 0.8 mWm^{-3} for the upper crust and 1.0
431 mWm^{-3} and 0.6 mWm^{-3} for the lower crust. The values reflect calculations of bulk crustal heat
432 production from the literature (Christensen and Mooney, 1995; Gao et al., 1998; Shaw et al.,
433 1986; Wedepohl, 1995). Changing the heat production for the upper and lower crust between
434 these extremes causes a small variation of 100 m in the tectonic subsidence. The heat production
435 of the bulk continental crust will be lower than that of accretionary crust and heat production
436 would have been higher during the Palaeozoic, so the model was also run with a higher heat
437 production of 2.0 mWm^{-3} (upper crust) and 1.2 mWm^{-3} (lower crust). This does reduce the
438 overall amount of tectonic subsidence from ~ 1800 to 1550m, but does not alter the timing. Fig.

1
2
3
4
5
6
7
8
9
10
11
12
13
14
15
16
17
18
19
20
21
22
23
24
25
26
27
28
29
30
31
32
33
34
35
36
37
38
39
40
41
42
43
44
45
46
47
48
49
50
51
52
53
54
55
56
57
58
59
60
61
62
63
64
65

439 6b shows that varying the heat production in the crust has a small effect compared to varying the
440 crustal thickness.

441 The other main parameter which has a big effect on the subsidence is the thickness of the
442 model, referred to as the plate thickness (Fig. 6c). A plate thickness of 95 km, which is the
443 preferred for the oceanic lithospheric cooling model of Stein and Stein (1992) results in 200 m
444 of subsidence, of which 80% has occurred within ~70 Myrs, with a final lithospheric thickness
445 (i.e. depth to the 1200 °C isotherm) of 81.1 km. At the other extreme when a plate thickness of
446 200 km is used, similar to an Archean craton (Priestley and McKenzie, 2006), ~3050 m of
447 subsidence is produced, and it takes longer for the subsidence to tail off. 80% of the subsidence
448 is completed within 200 Myrs. The lithosphere thickness after 500 Myrs is 166.5 km. As the
449 plate thickness is increased the final lithospheric thickness also increases. A thicker, dense
450 lithosphere results in more subsidence, occurring over a longer time period.

451 The temperature at the base of the plate is controlled by both the potential temperature at the
452 surface (the temperature at which the mantle adiabat dissects the surface) and the thickness of
453 the plate (Fig. 5). Increasing the potential temperature by 1°C increases the temperature at the
454 base of the plate by 1°C whereas increasing the thickness of the model causes the temperature at
455 the base of the plate to increase along the mantle adiabat i.e. 3°C for every 10 km. The potential
456 temperature was varied from 1280 °C, which was suggested by McKenzie et al. (2005) to 1410
457 °C suggested by Parsons and Sclater (1977). As Fig. 6d shows this variation of 100 °C in the
458 potential temperature produces less than 500 m difference in the overall subsidence.

459 Van Wees et al. (2009) report a trade off between parameters, such as the final lithospheric
460 thickness (plate thickness) and crustal thickness, when investigating the uncertainties in surface
461 heatflow using modelling. However, in this study we find that varying the plate thickness to fit

1
2
3
4
5
6
7
8
9
10
11
12
13
14
15
16
17
18
19
20
21
22
23
24
25
26
27
28
29
30
31
32
33
34
35
36
37
38
39
40
41
42
43
44
45
46
47
48
49
50
51
52
53
54
55
56
57
58
59
60
61
62
63
64
65

462 the time span of the subsidence and then varying the crustal thickness to fit the amount of
463 subsidence allows a unique solution to be obtained for these parameters. However, there is a
464 direct trade off between the crustal thickness, heat production and potential temperature because
465 they all only affect the total subsidence. The model is not sensitive to reasonable variations in
466 the heat production or potential temperature, but is sensitive to variations in crustal thickness
467 suggested for North Africa. Therefore the trade off between these parameters is not important
468 when trying to fit the modelled subsidence to the observed subsidence.

469 The sensitivity of the model to k , C_p and α was also investigated, but because much less is
470 known about the amount of variation that is found in the crust they are not discussed here and
471 the standard values from the literature (Fig. 5) are used. The forward model produces significant
472 subsidence for a large variety of crustal assemblages and for wide variation in the parameters. It
473 supports the hypothesis that lithospheric cooling and thickening caused the subsidence seen
474 across North Africa.

475
476 **5. Discussion**

477
478 *5.1 Comparison of tectonic subsidence from backstripping and forward modelling.*

479
480 The results of the forward modelling show a good fit to the backstripping from both basins as
481 demonstrated by Fig. 7. Four forward model runs are shown on the diagram. One of which uses
482 the best estimates for the crustal assemblage, thickness and plate thickness from the literature,
483 one which is the best fit to the backstripping and then two runs which show the maximum and
484 minimum subsidence for reasonable variations of the properties of the North African crust.

1
2
3
4 485 The forward model curves are smooth unlike the backstripped subsidence curves. This is
5
6 486 because North African crust has experienced periods of uplift, and the forward model doesn't
7
8
9 487 include these complexities. However, the forward model fits the broad shape of the backstripped
10
11 488 subsidence curve very well. Both have a concave up shape, and the timescale and magnitude of
12
13
14 489 subsidence are very similar. When the crustal thickness, final lithosphere thickness and heat
15
16 490 production used are taken from the best estimates of the North African crust in the literature
17
18
19 491 (Fig. 5), and therefore are independent of the backstripping, the forward model curve only
20
21 492 underestimates the subsidence slightly, by <500 m in 350 Myrs. The discrepancy at 500 Myrs is
22
23
24 493 ~700 m, because of the Mesozoic and Cenozoic subsidence of the Ghadames Basin. This is a
25
26 494 separate tectonic event, related to Tethyan opening and evolution (Guiraud and Bosworth,
27
28
29 495 1999). The best fit model has been fitted iteratively by eye. The input parameters for the best fit
30
31 496 model are the same as those from the literature except that the plate is 155 km thick, which
32
33 497 results in a final lithospheric thickness of ~124 km. The crust beneath the basins cannot be
34
35
36 498 assumed to be homogenous, in fact because it is accreted from numerous crustal fragments it is
37
38 499 likely that it varies across North Africa. The maximum and minimum subsidence based on the
39
40
41 500 variation found in the literature, discussed in section 4.2, is shown in Fig. 7. The upper limit has
42
43 501 a 35 km thick crust with 30 km of upper crust and 5 km of lower crust, a heat production of 1.6
44
45 502 mWm^{-3} in the upper crust and 1.0 mWm^{-3} in the lower crust, a potential temperature of 1280 °C
46
47
48 503 and plate thickness of 120 km. The lower limit has 25 km thick crust, where the top 5 km is
49
50
51 504 upper crust and the rest is lower crust, a heat production of 1.0 mWm^{-3} in the upper crust and 0.6
52
53 505 mWm^{-3} in the lower crust, a potential temperature of 1380 °C and a plate thickness of 180 km.

54
55 506 *Figure 7 should be placed here*
56
57
58
59
60
61
62
63
64
65

1
2
3
4
5
6
7
8
9
10
11
12
13
14
15
16
17
18
19
20
21
22
23
24
25
26
27
28
29
30
31
32
33
34
35
36
37
38
39
40
41
42
43
44
45
46
47
48
49
50
51
52
53
54
55
56
57
58
59
60
61
62
63
64
65

507 There are a number of assumptions in both the modelling and backstripping. Both are
508 oversimplified versions of the real situations and processes. The problem has been simplified to
509 be one dimensional, whereas the basins are three dimensional features. We assume that the
510 basins are large enough features that it is possible to remove effects of marginal uplift from the
511 sedimentary record by choosing wells away from the basin flanks, or constructing composite
512 wells. This allows the basins to be treated as one dimensional features. Another assumption is
513 that North African crust resembles the starting conditions outlined in the hypothesis. This is
514 difficult to test as there is no newly assembled accretionary orogenic belt on the North African
515 scale that can be used as an analogue. However, the building blocks of accretionary crust are
516 available to study. It seems reasonable that North African crust formed through subduction
517 would share the thin lithosphere of its component island arcs and accretionary wedges. When
518 North African crust is modelled using these starting conditions it produces a good fit to the
519 subsidence. As mentioned in the hypothesis as long as the crust is of near normal thickness and
520 has a thin mantle lithosphere these results still apply. The two North African basins have been
521 chosen as case studies, but we propose that the lithosphere cooling and thickening hypothesis is
522 applicable to all the Palaeozoic basins on the accretionary crust of North Africa and Arabia, and
523 to other basins on accretionary crust around the world, such as the Mesozoic cover of the
524 Scythian and Turan platforms of SW and Central Asia (Natal'in and Şengör, 2005), the
525 Mesozoic cover of the Tasmanides of Eastern Australia (Gallagher et al., 1994) and the late
526 Palaeozoic platform cover over the Altaid orogenic collage in Central Asia (Cook et al., 1994).

527 The good fit between modelled and backstripped subsidence curves do not prove that
528 lithosphere thickening and cooling is the cause of the subsidence. Other authors have suggested
529 that the Palaeozoic basins in North Africa formed by rifting (Lüning et al., 1999), orogenic

1
2
3
4
5
6
7
8
9
10
11
12
13
14
15
16
17
18
19
20
21
22
23
24
25
26
27
28
29
30
31
32
33
34
35
36
37
38
39
40
41
42
43
44
45
46
47
48
49
50
51
52
53
54
55
56
57
58
59
60
61
62
63
64
65

collapse (Ashwal and Burke, 1989) and dynamic topography (Heine et al., 2008). Lüning et al. (1999), compared the Al Kufrah Basin to pull apart basins in Oman and Saudi Arabia, and suggested that the Najd fault system may extend north into the Al Kufrah Basin and be reactivated as a rift during the Precambrian. Seismic lines of the south of the Al Kufrah Basin do indeed have features which have been interpreted as rifts. However, they are only found in a small area of the basin and the synrift subsidence accounts for a sixth of the overall subsidence (Ghanoush and Abubaker, 2007). The Ghadames Basin has very similar stratigraphy to Al Kufrah, but shows no evidence of rifting. Rifting is not widespread or large enough to cause the subsidence across all the Palaeozoic basins in North Africa. This also means that orogenic collapse is an unlikely subsidence mechanism, given that this is a special case of rifting on thickened continental crust. Armitage and Allen (2010) suggest that these basins can still form due to extension, but when stretching is occurring at low strain rates the strain might not localise along faults. It is hard to distinguish between their model and the model proposed in this paper on the grounds of rifting. Subsidence due to extension at low strain rates produces a period of constant subsidence during stretching followed by decreasing subsidence during the thermal sag phase. Whereas cooling of a thin lithosphere produces subsidence which decreases smoothly throughout time. The latter model fits the backstripping results (Fig. 4) which do not have a kink, but are be closer to a smooth curve.

There are problems with using dynamic topography to explain the basins: it has a transient effect and will rebound once the down welling has ceased leading to uplift and erosion. Nor is it possible at present to model whether the basins in North Africa would have been affected by mantle down-welling during the Palaeozoic. Thermal subsidence on the other hand explains the lateral extent of the subsidence as the lithosphere would be thin across most, if not all, of the

1
2
3
4 553 accretionary crust. Our results show that it is long lasting, fits the magnitude of the observed
5
6 554 subsidence and is able to cause subsidence over a wide range of terranes.

7
8
9 555 Thermal subsidence has a number of important implications. It suggests that one of the
10
11 556 fundamental properties of accretionary crust is that, in the absence of other competing tectonic
12
13
14 557 forces, it will subside after its formation. This will alter the overall composition of the crust,
15
16 558 adding several kilometres of sediments to crust made up largely of island arc and oceanic
17
18
19 559 material. It also predicts that the lithosphere beneath accretionary crust is not depleted by the
20
21 560 melting events which produced the crust, but is compositionally no different to upper mantle.
22
23
24 561 This will make the lithosphere more susceptible to thermal erosion as it does not have
25
26 562 compositional buoyancy and also affect the character of melts originating in it or passing
27
28
29 563 through it. Ashwal and Burke (1989) also noted that this fits the geophysical measurements of
30
31 564 the thickness and seismic properties of the lithosphere and with the geochemistry of Cenozoic
32
33 565 volcanism in North Africa.

34
35
36 566

37 38 567 **6. Conclusions**

39
40
41 568
42
43 569 We have shown that results from backstripping wells in two North African basins and
44
45 570 numerical modelling, are consistent with a basin forming mechanism of lithospheric cooling and
46
47
48 571 thickening, underneath relatively juvenile, accretionary crust. The backstripping revealed that
49
50
51 572 the Ghadames and Al Kufrah basins have experienced their highest rates of subsidence, (22.2
52
53 573 m/Myr and 10.1 m/Myr, respectively) at the start of the Palaeozoic, declining to almost zero at
54
55 574 the end of the Palaeozoic. There is almost no tectonic subsidence during the Mesozoic and
56
57
58 575 Cenozoic. The forward modelling shows that thermal subsidence of accretionary crust provides

1
2
3
4 576 a viable explanation for the formation of the Palaeozoic basins of North Africa, fitting the
5
6
7 577 available data better than previously suggested mechanisms.

8
9 578 We suggest that thermal subsidence following accretion would be expected in other areas of
10
11 579 accretionary crust, and could have influenced the rifted West Siberian Basin. It also predicts that
12
13
14 580 accretionary crust is underlain by fertile mantle lithosphere which may explain why Cenozoic
15
16 581 volcanism in North Africa and Arabia seems to originate from a fertile source (Ashwal and
17
18
19 582 Burke, 1989).

20
21 583
22 584 **Acknowledgements**

23
24
25 585 We thank Statoil for providing funding and well log data for the Ghadames Basin as well as
26
27 586 giving feedback and facilitating discussion with other researchers. We thank Philip Allen and an
28
29
30 587 anonymous reviewer for helpfully pointing out how the paper could be improved and focused.
31
32 588 We also thank Paul Ryan for his advice and input in early stages of the forward modelling.

33
34
35 589
36
37 590 **References**

- 38 591 Abadi, A.M., van Wees, J.-D., van Dijk, P.M., Cloetingh, S.A.P.L., 2008, Tectonics and
39 592 subsidence evolution of the Sirt Basin, Libya. AAPG Bulletin, 92, p. 993-1027.
40
41 593 Abdelsalam, M.G., Liégeois, J.P., Stern, R.J., 2002, The Saharan Metacraton, in: Fritz, H.,
42 594 Loizenbauer, J. (Eds.), 18th colloquium of African Geology J. of African Earth Sci. Graz
43 595 Austria, Elsevier, pp. 119-136.
44 596 Allen, P., Armitage, J.J., in press, Cratonic Basins, in: Busby, C.J., and Ingersoll, R.V. (Eds.),
45 597 Tectonics of sedimentary basins. Cambridge, Blackwell Science.
46
47 598 Allen, P.A., Allen, J., 2005, Basin Analysis. Principles and Applications. Oxford, Blackwell
48 599 Publishing.
49 600 Arcay, D., Doin, M.-P., Tric, E., Bousquet, R., de Capitani, C., 2006, Overriding plate thinning
50 601 in subduction zones: Localised convection induced by slab dehydration. *Geochem.*
51 602 *Geophys. Geosyst.*, 7, p. 26.
52
53 603 Armitage, J.J., Allen, P.A., 2010, Cratonic basins and the long-term subsidence history of
54 604 continental interiors: *J. of the Geol. Soc. of London*, 167, p. 61-70.
55 605 Artyushukov, E.V., 2005, The formation mechanism of the Barents Basin. *Russian Geology and*
56 606 *Geophysics*, 47, p. 683-696.
57
58 607 Ashwal, L.D., Burke, K., 1989, African lithospheric structure, volcanism and topography. *Earth*
59 608 *and Planetary Sci. Lett.*, 96, p. 8-14.

1
2
3
4
5
6
7
8
9
10
11
12
13
14
15
16
17
18
19
20
21
22
23
24
25
26
27
28
29
30
31
32
33
34
35
36
37
38
39
40
41
42
43
44
45
46
47
48
49
50
51
52
53
54
55
56
57
58
59
60
61
62
63
64
65

Bellini, E., Massa, D., 1980, A Stratigraphic contribution to the Paleozoic of the southern basins of Libya, in: Salem, M.J., Busrewil, M.T. (Eds.), The Geology of Libya, 2nd Symposium of the Geology of Libya, Volume 1. Amsterdam, Elsevier, p. 3-56.

Black, R., Latouche, L., Liégeois, J.P., Caby, R., Bertrand, J.M., 1993, Pan African displaced terranes in the Tuareg Shield (central Sahara). *Geology* 22, p. 641-644.

Boote, D.R.D., Clark-Lowes, D.D., Traut, M.W., 1998, Palaeozoic petroleum systems of North Africa, in: MacGregor, D.S., Moody, R.T.J., Clark-Lowes, D.D. (Eds.), *Petroleum Geology of North Africa: London, The Geological Society of London Special Publications No. 132*, p. 7-68.

Brunet, M.-F., Cloetingh, S.A.P.L., 2003, Integrated Peri-Tethyan basins studies (Peri-Tethys programme). *Sedimentary Geology*, 156, p. 1-10.

Bumby, A.J., Guiraud, R., 2005, The geodynamic setting of the Phanerozoic basins of North Africa: *J. of African Earth Sci.*, 43, p. 1-12.

Caby, R., 2003, Terrane assembly and geodynamic evolution of central-western Hoggar: a synthesis. *J. of African Earth Sci.*, 37, p. 133-159.

Capitanio, F.A., Faccenna, C., Funicello, R., 2009, The opening of the Sirte basin: Result of slab avalanching?. *Earth and Planetary Sci. Lett.*, 285, p. 210-216.

Christensen, N.I., Mooney, W.D., 1995, Seismic velocity structure and composition of the continental crust; a global view. *J. of Geophys. Res.*, 100, p. 9761-9788.

Cook, H.E., Zhemchuzhnikov, V.G., Buvtyshkin, V.M., Golub, L.Y., Gatovsky, Y.A., Zorin, Y.A., 1994, Devonian and Carboniferous passive-margin carbonate platform of southern Kazakhstan: Summary of depositional and stratigraphic models to assist in the exploration and production of coeval giant carbonate platform oil and gas fields in the north Caspian Basin, western Kazakhstan., in: Embry, A.F., Beauchamp, B., Glass, G.J. (Eds.), *Pangea: Global Environments and Resources*, Canadian Society of Petroleum Geologists Memoir 17, p. 363-381.

Craig, J., Rizzi, C., Said, F., Thusu, B., Lüning, S., Asbali, A.I., Keeley, M.L., Bell, J.F., Durham, M.J., Eales, M.H., Beswetherick, S., Hamblett, C., in press, Structural Styles and Prospectivity in the Precambrian and Paleozoic Hydrocarbon Systems of North Africa, *Geology of East Libya Symposium 2004*. Benghazi, p. 1-52.

Echikh, K., 1998, Geology and hydrocarbon occurrences in the Ghadames Basin, Algeria, Tunisia, Libya, in: MacGregor, D.S., Moody, R.T.J., Clark-Lowes, D.D. (Eds.), *Petroleum geology of North Africa*, Volume Special Publication No. 132. London, The Geological Society of London Special Publications, p. 109-129.

Elkins Tanton, L.T., Grove, T.L., Donnelly-Nolan, J., 2009, Hot, shallow mantle melting under the Cascades volcanic arc. *Geology*, 29, p. 631-634.

Fekirine, B., Abdallah, H., 1998, Palaeozoic lithofacies correlatives and sequence stratigraphy of the Saharan Platform, Algeria., in: MacGregor, D.S., Moody, R.T.J., Clark-Lowes, D.D. (Eds.), *Petroleum Geology of North Africa*, Volume Special Publications No. 132: London, The Geological Society of London Special Publications, p. 97-108.

Gallagher, K., Demitru, T.A., Gleadow, A.J.W., 1994, Constraints on the vertical motion of eastern Australia during the Mesozoic. *Basin Res.*, 6, p. 77-94.

Gao, S., Luo, T.-C., Zhang, B.-R., Zhang, H.-F., Han, Y.-w., Zhao, Z.-D., Hu, Y.-K., 1998, Chemical composition of the continental crust as revealed by studies in East China. *Geochimica et Cosmochimica Acta*, 62, p. 1959-1975.

1
2
3
4
5
6
7
8
9
10
11
12
13
14
15
16
17
18
19
20
21
22
23
24
25
26
27
28
29
30
31
32
33
34
35
36
37
38
39
40
41
42
43
44
45
46
47
48
49
50
51
52
53
54
55
56
57
58
59
60
61
62
63
64
65

Ghanoush, H., Abubaker, H., 2007, Gravity and Magnetic Profile along Seismic Intersect Ku - 89 - 04, Southern Kufra Basin - Libya, International Conference on Geo-resources in the Middle East and North Africa. Cairo University, Cairo.

Gorbatov, A., Dominguez, J., Suárez, G., Kostoglodov, V., Zhao, D., Gordeev, E., 1999, Tomographic imaging of the *P*-wave velocity structure beneath the Kamchatka peninsula. *Geophys. J. Int.*, 137, p. 269-279.

Grignani, D., Lanzoni, E., Elatrash, H., 1991, Paleozoic and Mesozoic subsurface of palynostratigraphy in the Al Kufra Basin, Libya, in: Salem, M.J., Hammuda, O.S., and Eliagoubi, B.A. (Eds.), *The Geology of Libya*, 3rd symposium of the Geology of Libya, Volume 4, Elsevier, p. 1159-1228.

Guiraud, R., Bosworth, W., 1999, Phanerozoic geodynamic evolution of northeastern Africa and the northwestern Arabian platform: *Tectonophysics*, 315, p. 73-108.

Guiraud, R., Bosworth, W., Thierry, J., Delplanque, A., 2005, Phanerozoic geological evolution of Northern and Central Africa. An overview: *J. of African Earth Sci.*, 43, p. 83-143.

Haq, B.U., Schutter, S.R., 2008, A chronology of Paleozoic sea-level Changes: *Science*, 322, p. 64-68.

Heine, C., Müller, R.D., Steinberger, B., Torsvik, T.H., 2008, Subsidence in intracontinental basins due to dynamic topography. *Physics of the Earth And Planetary Interiors*, 171, p. 252-264.

Holbrook, W.J., Lizarralde, D., McGeary, S., Bangs, N., Diebold, J., 1999, Structure and composition of the Aleutian Island Arc and implications for continental crustal growth. *Geology*, 27, p. 31-34.

Huang, J., Zhong, S., 2005, Sublithospheric small-scale convection and its implications for the residual topography at old ocean basins and the plate model. *J. of Geophys. Res.*, 110 (B8), doi:10.1029/2004JB003153.

Huang, J., Zhong, S., van Hunen, J., 2003, Controls on sublithospheric small-scale convection. *J. of Geophys. Res.*, 108 (B8), doi:10.1029/2003JB002456.

Janssen, M.E., Stephenson, R.A., Cloetingh, S.A.P.L., 1995, Temporal and spatial correlations between changes in plate motions and the evolution of rifted basins in Africa. *Geol. Soc. of America Bull.*, 107, p. 1317-1332.

Kaminski, E., Jaupart, C., 2000, Lithosphere structure beneath the Phanerozoic intracratonic basins of North America. *Earth and Planetary Sci. Lett.*, 178, p. 139-149.

Klein, G.D., 1995, Intracratonic Basins, in: Busby, C.J., Ingersoll, R.V. (Eds.), *Tectonics of Sedimentary basins*. Oxford, England, Blackwell Science, p. 459-478.

Kominz, M., 1995, Thermally subsiding basins and the insulating effect of sediment with application to the Cambro-Ordovician Great Basin sequence, western USA. *Basin Res.*, 7, p. 221-233.

Konert, G., Afifi, A.M., Al-Hajri, S.A., Groot, K.d., Naim, A.A.A., Droste, H.J., 2001, Paleozoic stratigraphy and hydrocarbon habitat of the Arabian Plate, in: Downey, M.W., Threet, J.C., Morgan, W.A. (Eds.), *Petroleum provinces of the twenty-first century*: Tulsa, United States, American Association of Petroleum Geologists, p. 483-515.

Le Heron, D.P., Armstrong, H.A., Wilson, C., Gindre, L., 2010, Glaciation and deglaciation of the Libyan Desert; the Later Ordovician record. *Sedimentary Geology*, 223, p. 100-125.

Lüning, S., Craig, J., Fitches, B., Mayouf, J., Busrewil, A., El Dieb, M., Gammudi, A., Loydell, D., McIlroy, D., 1999, Re-evaluation of the petroleum potential of the Kufra Basin (SE

- 1
2
3
4 699 Libya, NE Chad): does the source rock barrier fall?. *Marine and Petroleum Geology*, 16,
5 700 p. 693-718.
- 6 701 Macpherson, C.G., 2008, Lithosphere erosion and crustal growth in subduction zones: insights
7 702 from initiation of the nascent East Philippine Arc. *Geology*, 36, p. 311-314.
- 8 703 McKenzie, D., 1978, Some remarks on the development of sedimentary basins. *Earth and*
9 704 *Planetary Sci. Lett.*, 40, p. 25-32.
- 10 705 McKenzie, D., Jackson, J., Priestley, K., 2005, Thermal structure of oceanic and continental
11 706 lithosphere. *Earth and Planetary Sci. Lett.*, 233, p. 337-349.
- 12 707 Murphy, J.B., Nance, R.D., 1991, Supercontinent model for the contrasting character of late
13 708 Proterozoic orogenic belts *Geology*, 19, p. 469-472.
- 14 709 Natal'in, B.A., Şengör, A.M.C., 2005, Late Palaeozoic to Triassic evolution of the Turan and
15 710 Scythian platforms; the pre-history of the palaeo-Tethyan closure. *Tectonophysics*, 404,
16 711 p. 175-202.
- 17 712 Paquette, J.L., Caby, R., Djouadi, M.T., Bouchez, J.L., 1998, U-Pb dating of the end Pan-
18 713 African orogeny in the Tuareg shield: the post-collisional syn-shear Tiouéine pluton
19 714 (Western Hoggar, Algeria). *Lithos*, 45, p. 245-253.
- 20 715 Parsons, B., Sclater, J.G., 1977, An analysis of the variation of of the ocean floor bathymetry
21 716 and heat flow with age. *J. of Geophys. Res.*, 108, p. 803-827.
- 22 717 Pasyanos, M.E., Nyblade, A.A., 2007, A top to bottom lithospheric study of Africa and Arabia.
23 718 *Tectonophysics*, 444, p. 27-44.
- 24 719 Priestley, K., McKenzie, D., 2006, The thermal structure of the lithosphere from shear wave
25 720 velocities. *Earth and Planetary Sci. Lett.*, 244, p. 285-301.
- 26 721 Richter, F.M., Parsons, B., 1975, On the interaction of two scales of convection in the mantle. *J.*
27 722 *of Geophys. Res.*, 80, p. 2529-2541.
- 28 723 Ritzmann, O., Faleide, J.I., 2009, The crust and mantle lithosphere in the Barents Sea/Kara Sea
29 724 region. *Tectonophysics*, 470, p. 89-104.
- 30 725 Sclater, J.G., Christie, P.A.F., 1980, Continental stretching; an explanation of the post-Mid-
31 726 Cretaceous subsidence of the central North Sea basin. *J. of Geophys. Res.*, 85, p. 3711-
32 727 3739.
- 33 728 Seber, D., Sandvol, E., Sandvol, C., Brindisi, C., Barazangi, M., 2001, Crustal model for the
34 729 Middle East and North Africa region: implications for the isostatic compensation
35 730 mechanism. *Geophys. J. Int.*, 147, p. 630-638.
- 36 731 Selley, R.C., 1997, The basins of Northwest Africa; structural evolution, in: Selley, R.C. (Ed.),
37 732 *African basins: Sedimentary basins of the world: Amsterdam, Elsevier*, p. 17-26.
- 38 733 Şengör, A.M.C., Natal'in, B.A., Burtman, V.S., 1993, Evolution of the Altaid tectonic collage
39 734 and Palaeozoic crustal growth in Eurasia. *Nature*, 364, p. 299-307.
- 40 735 Şengör, A.M.C., Okurogullari, A.H., 1991, The role of accretionary wedges in the growth of
41 736 continents: Asiatic examples from Argand to Plate Tectonics. *Eclogae Geologicae*
42 737 *Helveticae*, 84, p. 535-597.
- 43 738 Shaw, D.M., Cramer, J.J., Higgins, M.D., Truscott, M.G., 1986, Composition of the Canadian
44 739 Precambrian shield and the continental crust of the earth, in: Dawson, J.B., Carson, D.A.,
45 740 Hall, J., Wedepohl, K.H. (Eds.), *The Nature of the Lower Continental Crust, Volume 24:*
46 741 *London, Geological Society of London Special Publications*, p. 275-282.
- 47 742 Stampfli, G.M., Borel, G.D., 2002, A plate tectonic model for the Paleozoic and Mesozoic
48 743 constrained by dynamic plate boundaries and restored synthetic oceanic isochrons. *Earth*
49 744 *and Planetary Sci. Lett.*, 196, p. 17-33.
- 50
51
52
53
54
55
56
57
58
59
60
61
62
63
64
65

- 1
2
3
4 745 Stein, C.A., Stein, S., 1992, A model for the global variation in oceanic depth and heat flow
5 746 with lithospheric age. *Nature*, 359, p. 123-129.
6
7 747 Stern, R.J., 1994, Arc assembly and continental collision in the Neoproterozoic East African
8 748 orogen: Implications for the consolidation of Gondwanaland. *Ann. Rev. of Earth and*
9 749 *Planetary Sci.*, 22, p. 319-351.
10 750 —, 2002, Subduction zones. *Rev. of Geophys.*, 40, doi:10.1029/2001RG000108
11 751 Sultan, M., Chamberlain, K.R., Bowring, S.A., Arvidson, R.E., Abuzied, H., Kaliouby, B.E.,
12 752 1990, Geochronologic and isotopic evidence for involvement of pre-Pan-African crust in
13 753 the Nubian Shield, Egypt. *Geology*, 18, p. 761-764.
14 754 Takahashi, N., Kodaira, S., Klemperer, S.L., Tatsumi, Y., Kaneda, Y., Suyehiro, K., 2007,
15 755 Crustal structure and evolution of the Mariana intra-oceanic island arc. *Geology*, 35, p.
16 756 203-206.
17
18 757 Turcotte, D.L., Schubert, G., 2002, *Geodynamics*. Cambridge, Cambridge University Press.
19 758 Turner, B.R., 1978, Paleozoic sedimentology of the south eastern part of the Al Kufrah Basin,
20 759 Libya: A model for oil exploration, in: Salem, M.J., Busrewil, M.T. (Eds.), *The Geology*
21 760 *of Libya*, 2nd symposium of the Geology of Libya, Volume 2, p. 351-375.
22
23 761 van Hunen, J., Zhong, S., Shapiro, N.M., Ritzwoller, M.H., 2005, New evidence for dislocation
24 762 creep from 3-D geodynamic modeling of the Pacific upper mantle structure. *Earth and*
25 763 *Planetary Sci. Lett.*, 238, p. 146-155.
26 764 van Keken, P.E., 2003, The structure and dynamics of the mantle wedge. *Earth and Planetary*
27 765 *Sci. Lett. Frontiers*, 215, p. 323-338.
28
29 766 Van Wees, J.-D., van Bergen, F., David, P., Nepveu, M., Beekman, F., Cloetingh, S.A.P.L.,
30 767 Bonté, D., 2009, Probabilistic tectonic heat flow modeling for basin maturation:
31 768 Assessment method and applications. *Marine and Petroleum Geology*, 26, p. 536-551.
32
33 769 Wedepohl, K.H., 1995, The composition of the continental crust. *Geochimica et Cosmochimica*
34 770 *Acta*, 59, p. 1217-1232.
35
36 771 Zhao, D., Hasegawa, A., Kanamori, H., 1994, Deep structure of Japan subduction zone as
37 772 derived from local, regional, and teleseismic events. *J. of Geophys. Res.*, 99, p. 22313-
38 773 22329.
39 774 Zor, E., Sandvol, E., Gürbüz, C., Türkelli, N., Seber, D., Barazangi, M., 2003, The Crustal
40 775 structure of the East Anatolian plateau (Turkey) from receiver functions. *Geophys. Res.*
41 776 *Lett.*, 30, p. 8044-8048.
42
43 777
44 778
45
46
47 779

48 780 **Figure Captions**

- 49
50 781
51
52
53 782 **Fig. 1.** Formation of accretionary crust and subsequent lithospheric thickening and subsidence. a) Assembly of
54 783 accretionary crust from island arcs and other crustal fragments through subduction. b) Newly formed accretionary
55 784 crust with a thinned lithosphere. c) Lithospheric thickening due to cooling causing subsidence.
56
57
58

59 785

1
2
3
4
5
6
7
8
9
10
11
12
13
14
15
16
17
18
19
20
21
22
23
24
25
26
27
28
29
30
31
32
33
34
35
36
37
38
39
40
41
42
43
44
45
46
47
48
49
50
51
52
53
54
55
56
57
58
59
60
61
62
63
64
65

Fig. 2. Present outcrop and sub-Mesozoic subcrop of Palaeozoic sediments across North Africa and Arabia (Boote et al., 1998; Konert et al., 2001). Four wells used to construct the Ghadames composite well are located along the line of the transect shown.

Fig. 3. Stratigraphy of the Ghadames and Al Kufrah basins used for backstripping analysis. The Ghadames composite well is constructed from four wells located along the transect shown in Fig. 2, to give the most complete sedimentary record. The locations of the wells from Al Kufrah are also marked on Fig 2.

Fig. 4. Tectonic subsidence curves for the Ghadames and Al Kufrah basins. The solid lines are the tectonic subsidence and the dotted lines show the subsidence if the stratigraphy is entirely shale or sandstone. This envelope is the maximum possible range of variation in the subsidence possible from varying the proportions of the lithologies.

Fig. 5. The right-hand side shows structure and initial temperature conditions for the numerical forward model. The solid line is the preferred temperature profile while the dashed line indicates the potential temperature. The left hand side shows the best estimates for the material properties for the different layers of crust and mantle from the literature. (Allen and Allen, 2005; Shaw et al., 1986; Turcotte and Schubert, 2002)

Fig. 6. The sensitivity of the forward model to variations **(a)** in the crustal thickness and proportion of lower crust (LC) and upper crust (UC), **(b)** the heat production, **(c)** the plate thickness and **(d)** the potential surface temperature of the mantle adiabat.

Fig. 7. Comparison of the subsidence from backstripping the composite well from the Ghadames Basin with a range of forward model runs. The hypothesised subsidence mechanism fits the observed subsidence well although there is a wide range of subsidence over the possible range of variations in the North African crust as demonstrated by the upper and lower limits.

1
2
3
4
5
6
7
8
9
10
11
12
13
14
15
16
17
18
19
20
21
22
23
24
25
26
27
28
29
30
31
32
33
34
35
36
37
38
39
40
41
42
43
44
45
46
47
48
49
50
51
52
53
54
55
56
57
58
59
60
61
62
63
64
65

813 **Table Captions**

814

815 **Table 1** Compilation of intracratonic basins situated on accretionary crust from around the world. The table shows
816 their locations and the temporal link between the end of the accretion event forming the underlying crust and the
817 beginning of subsidence across the basin as a whole.

Table 1[Click here to download Table: Table 1.doc](#)

Basin Name	End of basement accretion	Beginning of platformal subsidence
<i>South America</i>	~510 Ma (Cordani and Teixeira, 2007)	
Parnaíba Basin		Silurian (Oliveira and Mohriak, 2003) \leq 444 Ma
Paraná Basin		Ordovician (Brito Neves, 2002; Zalán et al., 1990) \leq 488 Ma
Choco-Paraná Basin		Ordovician (Brito Neves, 2002) \leq 488 Ma
<i>North Africa</i>	~550 Ma (Caby, 2003)	
Mouydir Basin		Cambrian (Boote et al., 1998) \leq 542 Ma
Ahnet Basin		Cambrian (Boote et al., 1998) \leq 542 Ma
Reggane Basin		Cambrian (Boote et al., 1998) \leq 542 Ma
Ghadames Basin		Cambrian (Boote et al., 1998) \leq 542 Ma
Al Kufrah Basin		Cambrian (Boote et al., 1998) \leq 542 Ma
<i>South Africa</i>	~550 Ma (Bumby and Guiraud, 2005)	
Cape Basin		Cambrian (Tankard et al., 2009) \leq 542 Ma
<i>Arabia</i>	~550 Ma (Stern, 1994)	
Arabian Platform		Cambrian (Konert et al., 2001) \leq 542 Ma
<i>Central Asia</i>	~210 Ma (Natal'in and Şengör, 2005)	
Scythian Platform		Jurassic (Natal'in and Şengör, 2005) \leq 200 Ma
Turan Platform		Jurassic (Natal'in and Şengör, 2005) \leq 200 Ma
<i>Eastern Australia</i>	~250 Ma (Glen, 2005)	
Eromanga Basin		Jurassic (Gallagher et al., 1994) \leq 200 Ma
Surat Basin		Jurassic (Gallagher et al., 1994) \leq 200 Ma

Figure 1
[Click here to download high resolution image](#)

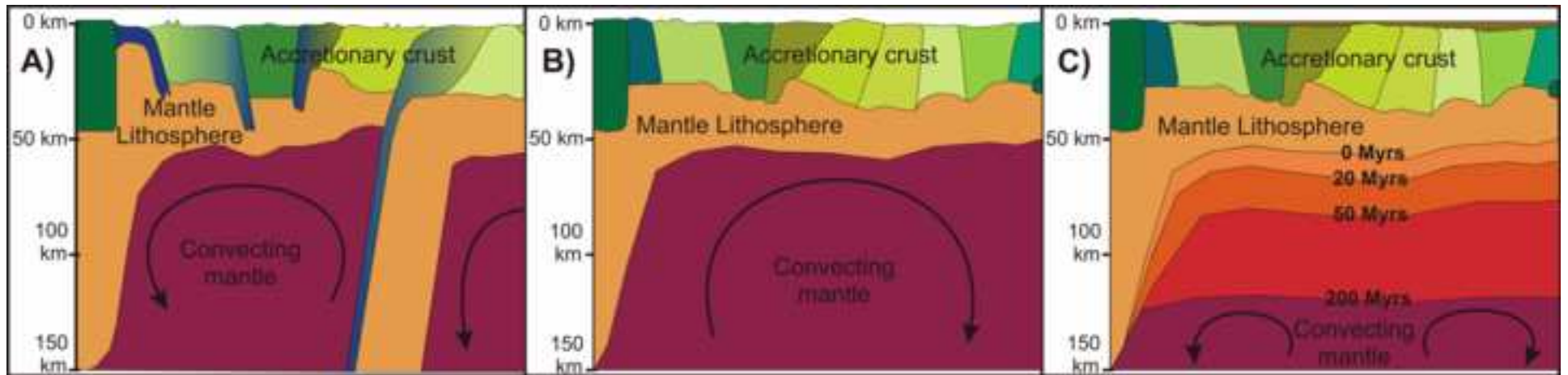


Figure 2
[Click here to download high resolution image](#)

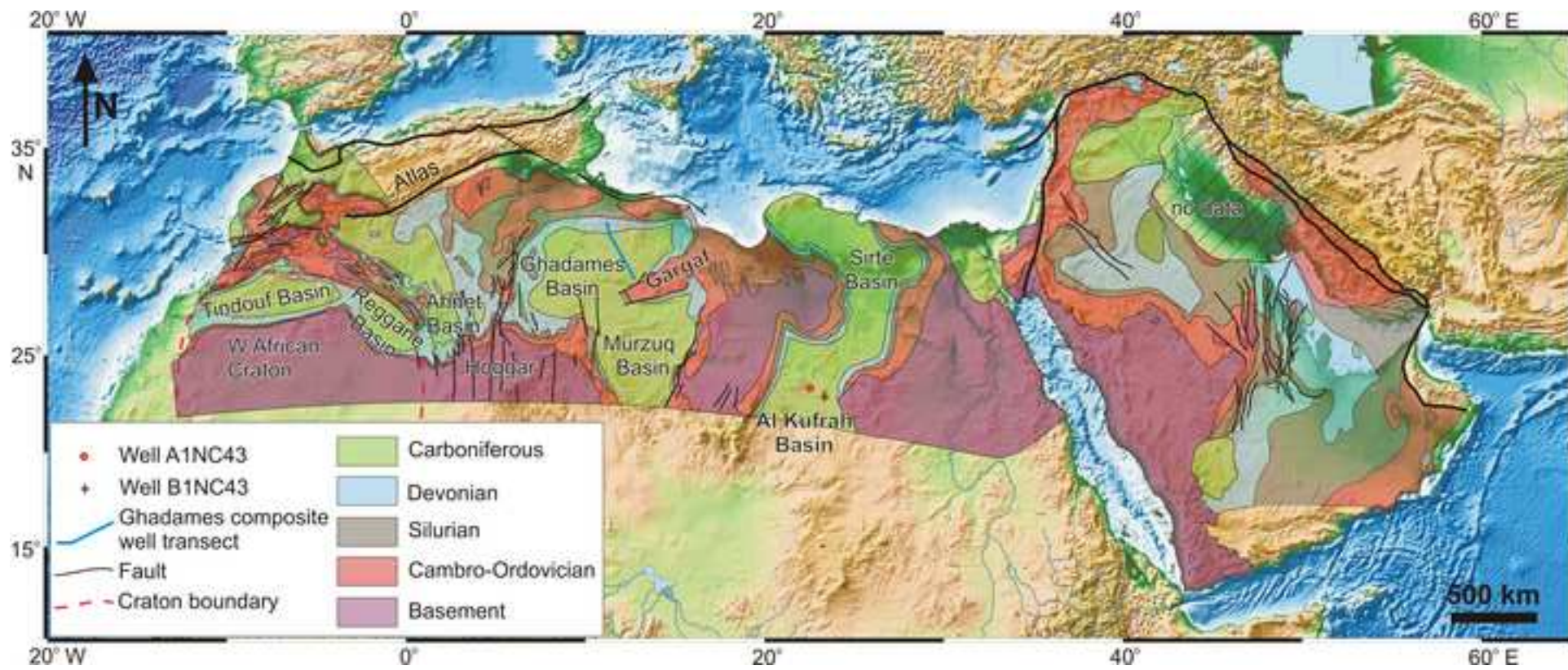
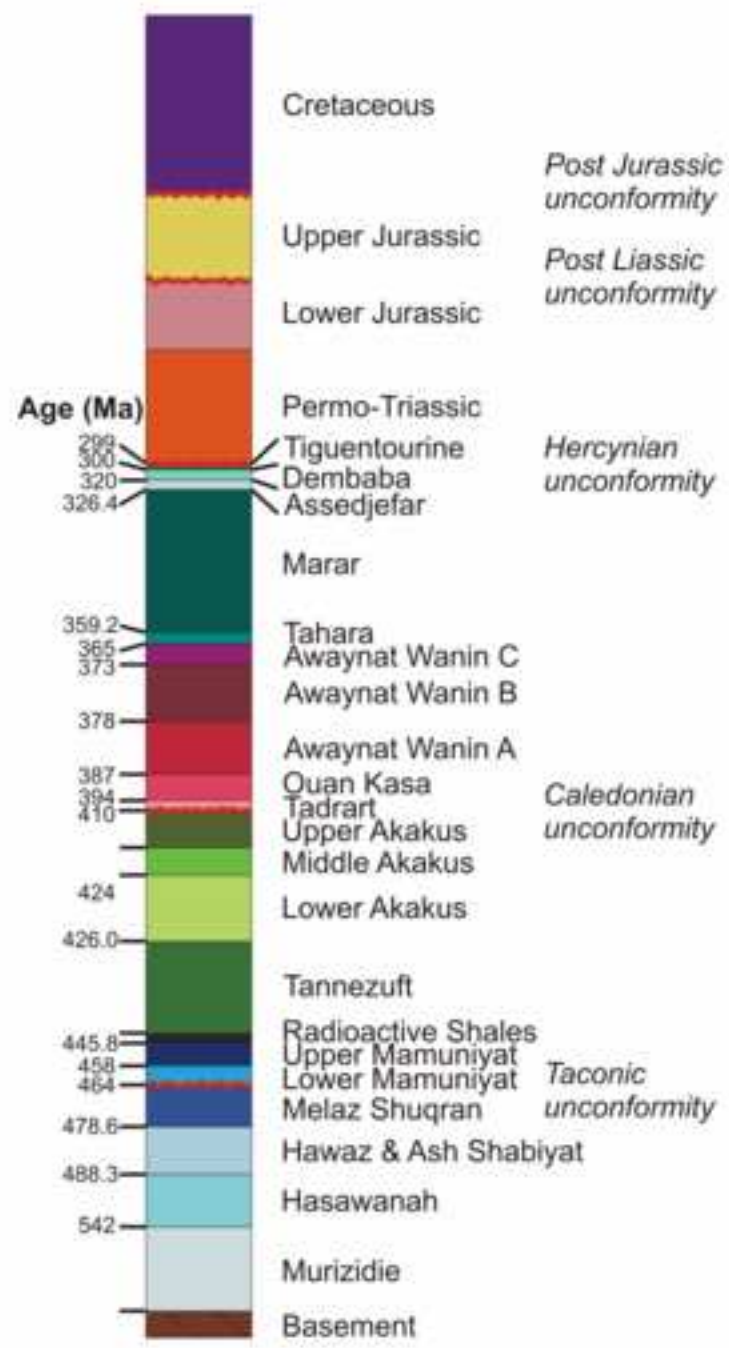
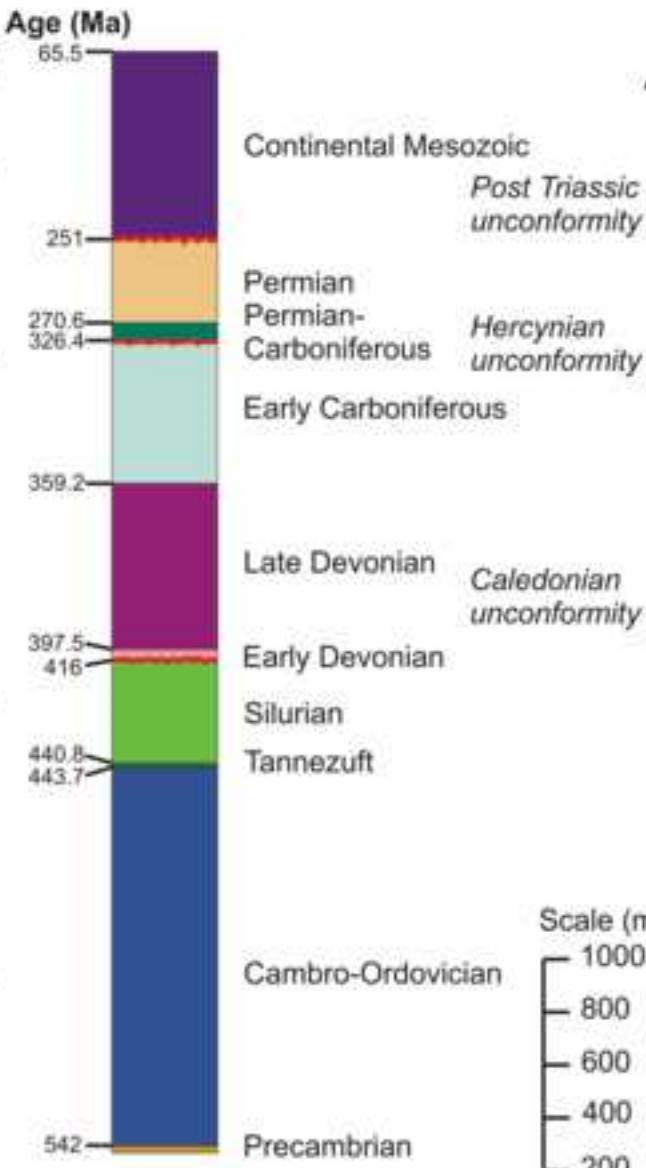


Figure 3
[Click here to download high resolution image](#)

Ghadames Composite Well



Well B1NC43 Al Kufrah



Well A1NC43 Al Kufrah

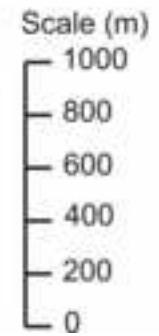
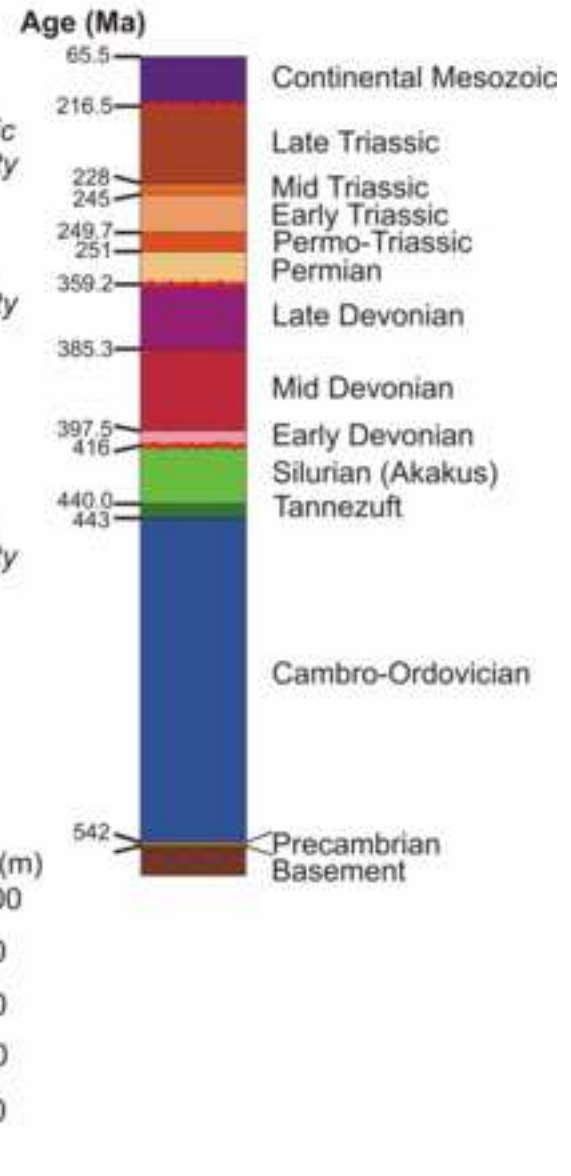


Figure 4

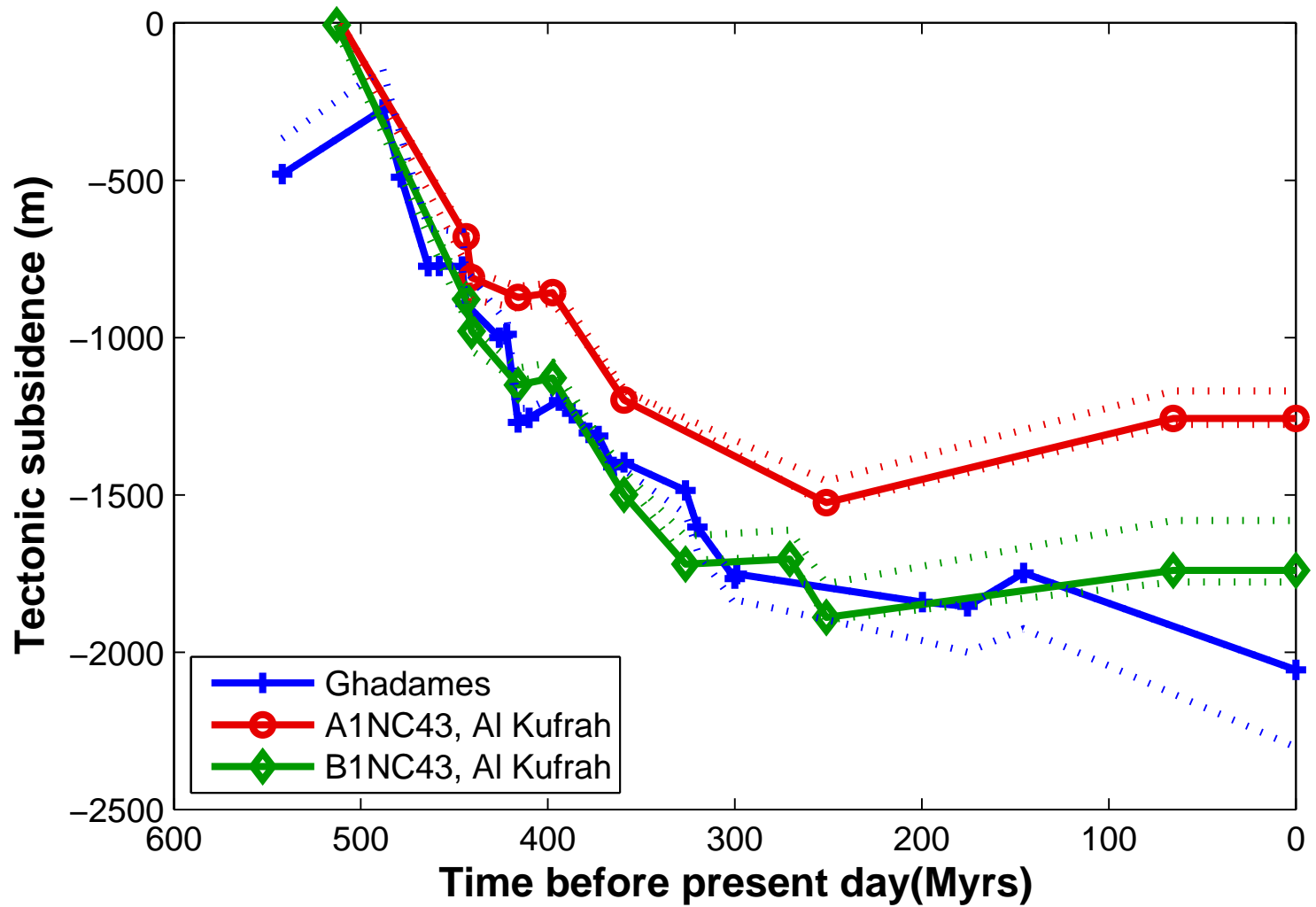
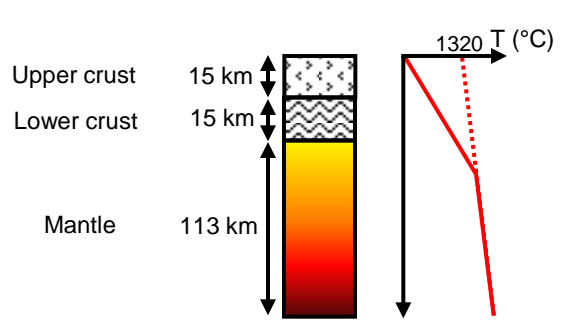


Figure 5



ρ_0 (kgm ⁻³)	A (mWm ⁻³)	α (K ⁻¹)	k (Wm ⁻¹ K ⁻¹)	Cp (Jkg ⁻¹ K ⁻¹)
2750	1.31	2.4×10^{-5}	3.1	790
2900	0.8	1.6×10^{-5}	2.1	790
3300	0.006	3.3×10^{-5}	3.3	790

Figure 6 Black and White version

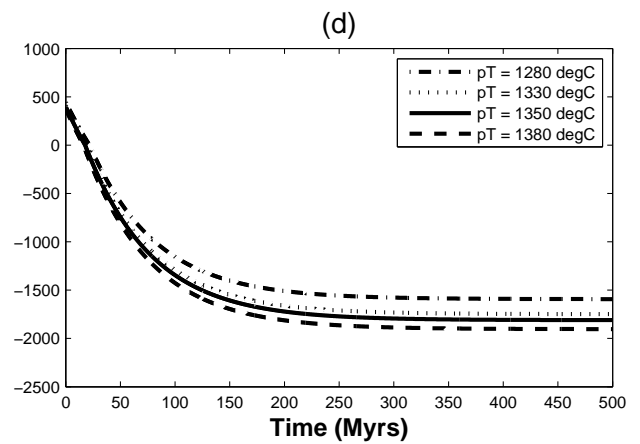
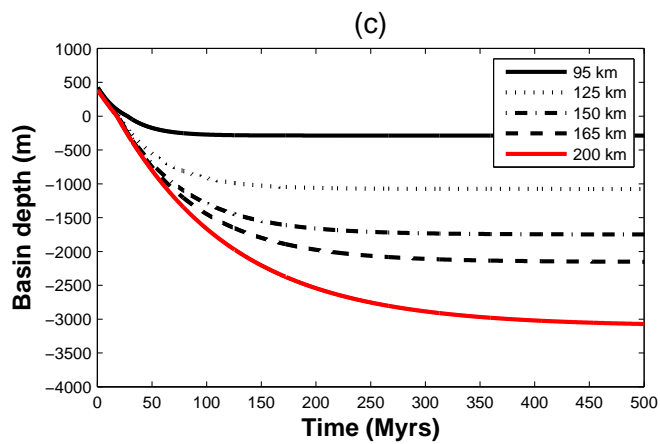
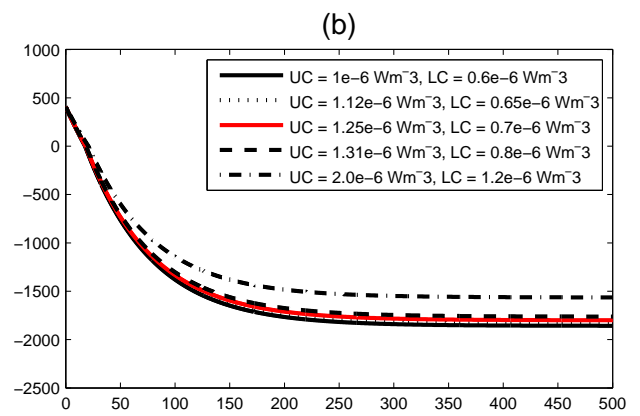
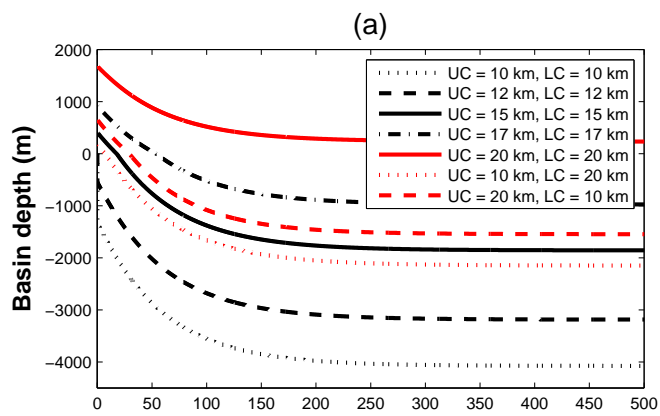


Figure 6 Colour version

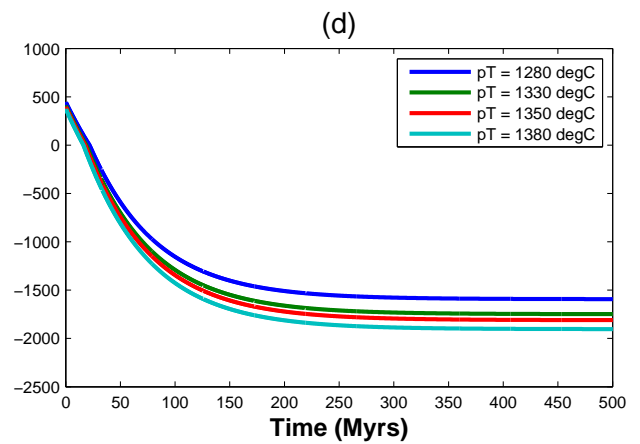
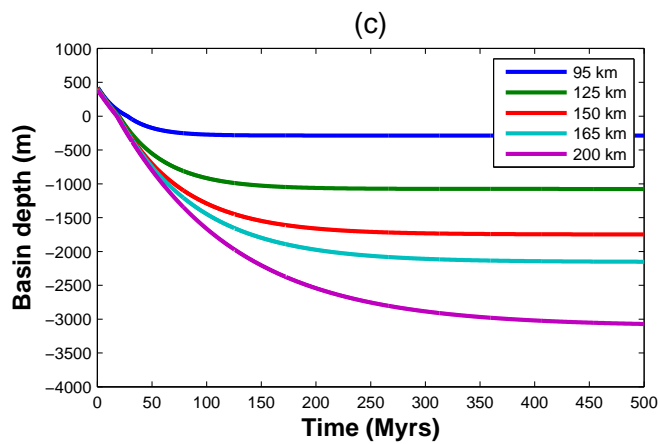
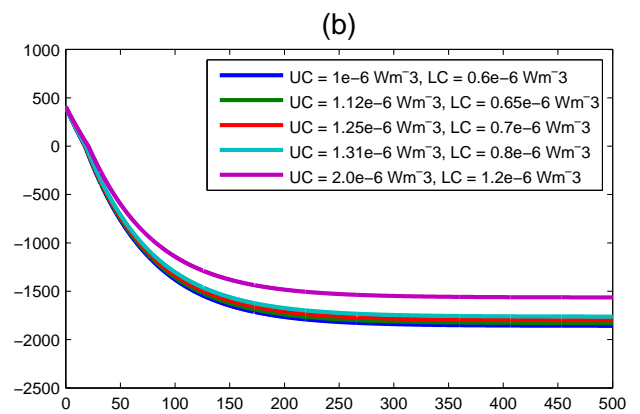
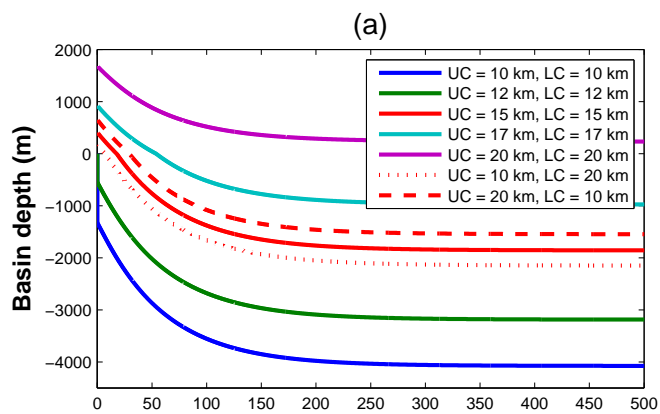


Figure 7

